A&A 624, A143 (2019)
https://doi.org/10.1051/0004-6361/201629162

Astronomy & Astrophysics

Highly luminous supernovae associated with gamma-ray bursts

I. GRB 111209A/SN 2011kl in the context of stripped-envelope and superluminous supernovae*

D. A. Kann[1,2,3,4], P. Schady[2], F. Olivares E.[5], S. Klose[1], A. Rossi[6,1], D. A. Perley[7,8,9], T. Krühler[2,8,10], J. Greiner[2,3], A. Nicuesa Guelbenzu[1], J. Elliott[2,11], F. Knust[2], R. Filgas[12], E. Pian[5,13], P. Mazzali[14,15], J. P. U. Fynbo[8], G. Leloudas[16,8], P. M. J. Afonso[17], C. Delvaux[2], J. F. Graham[2], A. Rau[2], S. Schmidl[1], S. Schulze[18,19,20], M. Tanga[2], A. C. Updike[21], and K. Varela[2]

(Affiliations can be found after the references)

Received 22 June 2016 / Accepted 4 March 2019

ABSTRACT

Context. GRB 111209A, one of the longest gamma-ray bursts (GRBs) ever observed, is linked to SN 2011kl, which is the most luminous GRB supernova (SN) detected so far. Several lines of evidence indicate that this GRB-SN is powered by a magnetar central engine.
Aims. We place SN 2011kl into the context of large samples of SNe, addressing in more detail the question of whether this GRB-SN could be radioactively powered, and whether it represents an extreme version of a GRB-SN or an underluminous superluminous SN (SLSN).
Methods. We modelled SN 2011kl using SN 1998bw as a template and derived a bolometric light curve including near-infrared data. We compared the properties of SN 2011kl to literature results on stripped-envelope and SLSNe.
Results. A comparison in the k, s context, i.e. comparing SN 2011kl to SN 1998bw templates in terms of luminosity and light-curve stretch, clearly shows SN 2011kl is the most luminous GRB-SN to date and is spectrally very dissimilar to other events because it is significantly bluer/hotter. Although SN 2011kl does not reach the classical luminosity threshold of SLSNe and evolves faster than any of these objects, it resembles SLSNe more than the classical GRB-associated broad-lined Type Ic SNe in several aspects.
Conclusions. GRB 111209A was a very energetic event, both at early (prompt emission) and at very late (SN) times. We show in a companion publication that with the exception of the extreme duration, the GRB and afterglow parameters are in agreement with the known distributions for these parameters. SN 2011kl, on the other hand, is exceptional both in luminosity and spectral characteristics, indicating that GRB 111209A was likely not powered by a standard-model collapsar central engine, further supporting our earlier conclusions. Instead, it reveals the possibility of a direct link between GRBs and SLSNe.

Key words. gamma-ray burst: individual: 111209A – supernovae: individual: 2011kl – stars: neutron

1. Introduction

Gamma-ray bursts (GRBs) are the most luminous explosions in the Universe (see e.g. Gehrels et al. 2009 for a recent review). Their afterglow emission can be extremely luminous during and right after the GRB (Kann et al. 2007; Racusin et al. 2008; Bloom et al. 2009). There are at least two classes of GRBs (Mazets et al. 1981; Kouveliotou et al. 1993). The class generally known as long GRBs, or Type II GRBs in a more physically motivated classification scheme which is independent of duration, (Gehrels et al. 2006; Zhang et al. 2007, 2009; Kann et al. 2010, 2011) has been shown to be conclusively linked to the supernovae (SNe) explosions of very massive stars (e.g. Galama et al. 1998; Hjorth et al. 2003; Stanek et al. 2003, see e.g. Cano et al. 2017a for a review, and Barnes et al. 2018 for numerical modelling). These stars are likely Wolf–Rayet stars, which are thought to be linked to Type Ic SNe, the explosions of highly stripped massive stellar cores which have either ejected (via binary interaction up to common-envelope phases, e.g. Fryer & Heger 2005; Sana et al. 2012) or burned (via chemically homogeneous evolution, e.g. Yoon & Langer 2005) their H and He envelopes (see e.g. Smartt 2009 for a review). The advent of untargeted automatic sky surveys has led to the discovery of large numbers of these so-called stripped-envelope SNe (e.g. Taddia et al. 2018, 2019a; Stritzinger et al. 2018a,b), allowing statistically significant studies of the distributions of luminosity or rise/decay times, spectral characteristics (e.g. the question of He in Type Ic spectra), expansion speeds, produced ^{56}Ni masses, ejecta kinetic energies, and more. We note that Sobacchi et al. (2017a) posited that the existence of a He layer prevents jet breakout, therefore GRBs are not associated with Type Ib SNe. Such highly stripped SNe generally exhibit very high expansion velocities of $\approx 0.1c$ (e.g. Bufano et al. 2012; Schulze et al. 2014; Izzo et al. 2019), leading to the term "broad-lined Type Ic SNe" (henceforth Type Ic-BL SNe). Recently, Prentice & Mazzali (2017) presented a physically motivated classification of SE-SNe, in which they found that all GRB-SNe are Type Ic-3; conversely, not all Type Ic SNe with high expansion speeds are associated with GRBs and almost all of these non-GRB SNe have $N > 3$ in the classification scheme of Prentice & Mazzali (2017). In rare cases, such Type Ic-BL SNe show evidence for relativistic ejecta but without an associated GRB, for example SN 2009bb (Soderberg et al. 2010; Pignata et al. 2011), SN 2012ap (Margutti et al. 2014; Milisavljevic et al. 2015a), and iPTF17cw (Corsi et al. 2017), the latter possibly being associated with a GRB.

* Partially based on observations obtained under programme 088.A-0051(C), PI: J. P. U. Fynbo.

The GRB 111209A, discovered by the *Neil Gehrels Swift* Observatory satellite (Gehrels et al. 2004), is a truly remarkable event, at 25 ks the second-longest (after GRB 170714A; D'Ai et al. 2017; Kann et al. 2017) GRB ever discovered (Golenetskii et al. 2011; Gendre et al. 2013), and one of the very rare ultra-long GRBs (ULGRBs; Levan et al. 2014; henceforth L14; see also Levan 2015). Using the GROND instrument (Greiner et al. 2008), we discovered that GRB 111209A was accompanied by a very luminous SN (Greiner et al. 2015, henceforth G15), dubbed SN 2011kl, which is the most luminous GRB-SN discovered so far, and spectrally dissimilar to any known GRB-SN because it is much bluer and hotter and exhibits a spectrum much more in accordance with those of superluminous supernovae (SLSNe; G15, Mazzali et al. 2016; Liu et al. 2017b). The afterglow of GRB 111209A shows a complex evolution but is generally unremarkable within the context of GRB afterglows (Stratta et al. 2013; Kann et al. 2018; henceforth K18B).

In this paper, we build upon our earlier results (G15; K18B). We derive a bolometric light curve of SN 2011kl incorporating an IR correction, which had not been undertaken by G15. Using both our own extensive GRB-SN analysis (Kann et al., in prep.) and large samples derived from the literature, we place SN 2011kl in context and study whether this is an extreme GRB-SN or is more similar to SLSNe, which would establish a direct connection between the most luminous SNe and the most luminous high-energy transients.

The paper is organized as follows: In Sect. 2 we present our fit to the late-time data of the afterglow of GRB 111209A (further to the analysis and results of G15 and K18B) and the derivation of the parameters of SN 2011kl as well as the bolometric light curve. In Sect. 3 we present results on the blackbody fits of the SN emission and the absolute magnitudes of the SN. In Sect. 4, we place SN 2011kl into the context of GRB-SNe, other SE-SNe and SLSNe, and we discuss the nature of GRB 111209A/SN 2011kl in the light of our combined results. We reach our conclusions in Sect. 5.

We follow the convention $F_\nu \propto t^{-\alpha}\nu^{-\beta}$ to describe the temporal and spectral evolution of the afterglow. We use WMAP ΛCDM concordance cosmology (Spergel et al. 2003) with $H_0 = 71\,\mathrm{km\,s^{-1}\,Mpc^{-1}}$, $\Omega_\mathrm{M} = 0.27$, and $\Omega_\Lambda = 0.73$. Uncertainties are given at 68% (1σ) confidence level for one parameter of interest unless stated otherwise, whereas upper limits are given at the 3σ confidence level.

2. Fitting SN 2011kl

Using a combination of our unique GROND data set along with crucial data from the literature, G15 for the first time found evidence for both a jet break and a late-time SN component for this GRB. This jet break is actually hidden by the rising SN in all filters except U. We also note we have a data gap between 13 and 22 days that is larger on the logarithmic scale than the time between other data points because of a period of bad weather. We may therefore have missed a steeper decay component during this time. The consensus in the literature prior to the publication of our results in G15 had been that this GRB exhibited the lack of an associated SN, which drove much of the interpretation and modelling of the data that had been published at that time (Gendre et al. 2013; L14; Stratta et al. 2013; Kashiyama et al. 2013; Nakauchi et al. 2013, see Sect. 4.2). Our detection therefore constituted a paradigm shift. We describe the fitting procedure in detail in the following.

2.1. Fitting the late afterglow and the supernova

The GROND/UVOT data of the afterglow of GRB 111209A were given in K18B, where we also present the data analysis and the complete analysis of the early afterglow. From ≈6 days to ≈10 and possibly even ≈13 days, the afterglow decays monotonically and achromatically before showing a strong departure from this behaviour at >20 days. This so-called "late red bump" is a characteristic sign of a late-time SN contribution to the optical transient following a GRB (e.g. Price et al. 2003). In the *white* data as well as the $F336W/u'$ data from L14, the afterglow is seen to decay more rapidly.

Such bumps were already found in the very first afterglows, such as for GRB 970228 (Galama et al. 2000) and GRB 980326 (Bloom et al. 1999). These bumps were studied systematically by Zeh et al. (2004), who came to the conclusion that all afterglows of GRBs at $z \leq 0.7$ (as well as some in the range $0.7 \leq z \leq 1.1$) showed evidence of a late-time SN contribution. Depending on the evolution of the afterglow, these bumps are more or less easy to detect. In case of an afterglow with an early break, a steep decay, and a faint (or well-subtracted) host contribution, the bumps are very prominent (e.g. GRB 011121: Garnavich et al. 2003; Greiner et al. 2003; GRB 020405: Price et al. 2003; Masetti et al. 2003; GRB 041006: Stanek et al. 2005). If the afterglow decay is less steep, this results in a transition to a plateau phase which can be mistaken for the constant host galaxy contribution, but shows a further drop after ≈50 . . . 100 days (e.g. GRB 050525A: Della Valle et al. 2006; GRB 090618: Cano et al. 2011; GRB 091127: Cobb et al. 2010; Filgas et al. 2011; Vergani et al. 2011). Finally, in case of a distant GRB with a host galaxy of similar magnitude (e.g. GRB 021211: Della Valle et al. 2003) or a bright, slowly decaying afterglow (e.g. GRB 030329: Kann et al. 2006; X-ray flash (XRF) 050824: Sollerman et al. 2007; GRB 060729: Cano et al. 2011), the contribution of the SN can be hard to decipher.

We perform the SN fitting together with that of the late afterglow with the method of Zeh et al. (2004) and give the results in the k, s formalism (see below). Those authors used the light curves of SN 1998bw as given by Galama et al. (1998) as a template, and derived an analytical equation which is able to fit the data well (Klose et al. 2019). We create SN 1998bw template light curves in the GROND bandpasses (as well as J from L14) and at the redshift of GRB 111209A, i.e. the resulting light curves show what SN 1998bw would look like at $z = 0.677$ if observed with GROND/HAWK-I J. These templates are fitted with the above-mentioned analytical equation, which can then be used to perform nonlinear curve fitting using χ^2 minimization on the data of GRB 111209A. The SN 1998bw template is unique in each bandpass and described by a set of seven parameters, which are different depending on the bandpass and (in case of other GRBs) the redshift (Zeh et al. 2004). The entire fit uses a joint afterglow model with a single decay index but five differently scaled templates for the SN fitting; there is no more significant evidence for chromatic behaviour as is seen in the rebrightening (see K18B). These templates are additionally modified by the k and s values. The luminosity factor k describes how luminous the GRB-SN is relative to SN 1998bw itself, i.e. it scales the entire light curve up and down. The stretch factor s is simply a multiplicative factor applied to the time axis, while we assume the general behaviour of the light curve remains identical (and the SN evolution initializes at the time of the GRB itself), i.e. s is able to make the evolution faster or slower than SN 1998bw, which by definition has $k = 1, s = 1$. So far, while GRB-SNe have been found that evolve considerably faster than SN 1998bw

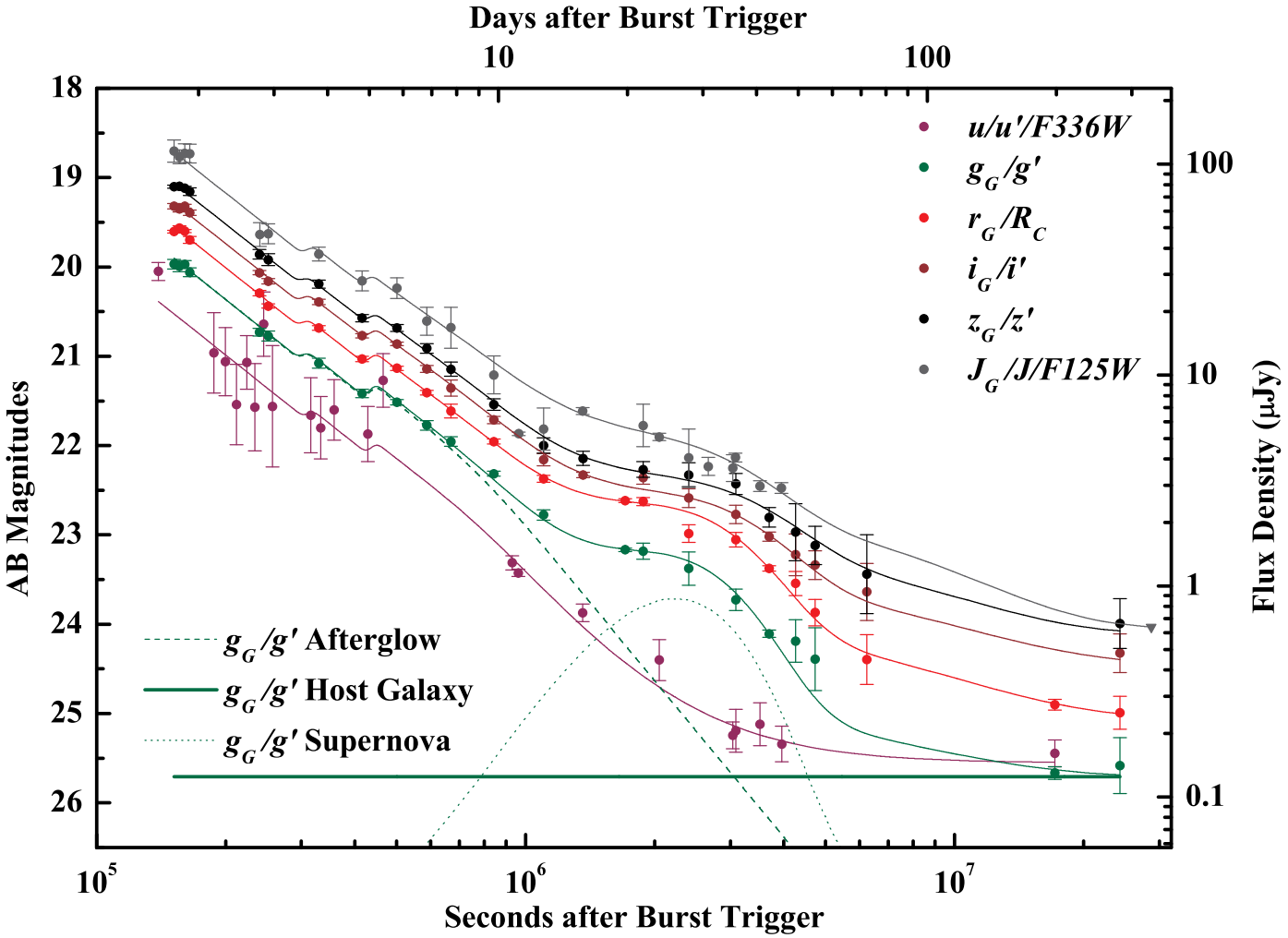

Fig. 1. Late light curve of the optical/NIR afterglow of GRB 111209A in $Ug'r'i'z'J$ fit (U being UVOT u, SDSS u' and HST $F336W$) with the combination of a broken power-law afterglow component (including two steps at earlier times), a SN component based on the SN 1998bw template, and a late-time host-galaxy value. The U light curve does not incorporate a SN and has been used to determine the (jet) break time and post-break decay slope. The full line is the fit to each colour. For the g' band, we additionally show the decomposition into afterglow, host galaxy, and SN component. The fit shown is identical to that given in G15; we show the best-fit curves for all filters.

(Ferrero et al. 2006; Sollerman et al. 2007; Olivares et al. 2012) and also considerably slower (Stanek et al. 2005), none have showed significant deviations from the template shape, thereby validating the formalism. This is definitely not true for Type Ic SNe in general, even BL Type Ic SNe not associated with GRBs; see the appendix of Ferrero et al. (2006).

The afterglow and SN phase are excellently covered by GROND in $g'r'i'z'$, but the SN is not detected in $J_{\rm GROND}$. Therefore, we add VLT/J and HST/$F125W$ data from L14, except for the first HST $F125W$ point, which is anomalously faint (see Fig. 1 at 960 ks, on the i'-band fit curve). The L14 authors also presented two epochs of $g'R_Ci'z'$ data during the SN phase, which agree excellently with our data, as L14 used our GROND calibration stars. Finally, the most important contributions from L14 are late-time u' and HST $F336W$ data. These authors found a decay slope of $\alpha = 1.38$ from combined UVOT u and their $u'F336W$ data. This value is in decent agreement with our values determined from our joint afterglow fit, but L14 fit a single power-law to data from ≈1−50 days. Their error while performing this fit lies in ignoring a host-galaxy contribution; the data at ≈30−50 days is already on the level of the host galaxy (which is actually noted in their work). Taking this into account, we see clear evidence for a steeper afterglow decay at late times. As discussed in more detail in Sect. 4.1, we do not expect a SN contribution at this redshift in this wavelength range, which is also fully validated by the SN spectrum (G15); therefore we use these data as a template for the pure afterglow contribution. To obtain a good fit, we combine UVOT u, Gemini u', and HST $F336W$ data into one light curve[1]. While these filters differ slightly, the data are dominated by statistical errors, so we do not expect small filter mismatches to affect the result as long as all values are in AB magnitudes. To obtain the best possible value for the pre-break afterglow slope, we use data starting at the second GROND epoch (the beginning of the post-rebrightening decay), taking the two step-like rebrightenings into account and fixing the decay slope to be identical in all three segments; this is motivated by our interpretation of these features (see K18B) and we find no evidence for a strong discrepancy compared to the null hypothesis of a single decay slope. Finally, we add a filter-dependent host-galaxy component at very late times, both from our data (see K18B for further discussion of the host galaxy) and

[1] We refer to this wavelength range as U from now on; it is roughly analogous to the rest-frame UVOT $uvw2$ band at 1928 Å.

Table 1. Results of the SN fit.

Filter	$\lambda_{\rm rest}$ (Å)	$m_{\rm k}$	k	s
U	2138	22.955 ± 0.112	...	...
g'	2735	22.286 ± 0.099	4.97 ± 0.49	1.26 ± 0.02
r'	3709	21.970 ± 0.097	3.14 ± 0.27	1.13 ± 0.02
i'	4556	21.713 ± 0.096	1.81 ± 0.22	1.12 ± 0.05
z'	5360	21.544 ± 0.098	1.71 ± 0.25	1.05 ± 0.08
J	7394	21.146 ± 0.102	3.59 ± 0.33	0.79 ± 0.03

Notes. These results are based on a joint fit of all bands showing a SN component and the U band from which we derive the pure afterglow parameters. See text for more details.

from L14; we use their HST $F336W$ value for the U band. The complete fit therefore consists of the following components and parameters:

– An afterglow component, described by a broken power-law, which has a pre-break decay slope $\alpha_{\rm late,1}$, post-break decay slope $\alpha_{\rm late,2}$, break time $t_{\rm b}$ and break smoothness n as shared parameters for all filters, while the normalization $m_{\rm k}$ (magnitude at $t_{\rm b}$ assuming $n = \infty$) is an individual parameter for each filter.
– A SN component, in all bands except U, which has a luminosity factor k and stretch factor s being individual parameters for each filter.
– A host galaxy component, individual for each filter, for J, we use the upper limit from L14, which we independently confirmed as a maximum possible host value.

Our fit result is shown in Fig. 1. Because of some scatter in the data (e.g. the early UVOT u data), the fit is not satisfactory ($\chi^2 = 143.5$ for 109 degrees of freedom). For the afterglow, we find $\alpha_{\rm late,1} = 1.55 \pm 0.01$, $\alpha_{\rm late,2} = 2.33 \pm 0.16$, $t_{\rm b} = 9.12 \pm 0.47$ days, and $n = 10$ has been fixed. The parameters for the SN are given in Table 1. This fit was also used in G15.

The only other study which has presented late-time observations is L14. While they have data during the SN phase which is, as pointed out further above, in excellent agreement with our own, they lack high S/N observations of the afterglow between ≈1 day (where they have further Gemini observations, a single epoch in several colours during the steep rise) and the time when the SN dominates. This leads to fits with different decay slopes (in U and J; see their Fig. 6), an inability to clearly separate the afterglow and SN components, and only weak constraints on a jet break. In their work, L14 present several tantalizing hints towards the existence of the SN. First, they find clear reddening at late times in comparison to their earlier data. Secondly, next to early VLT/X-shooter and Gemini/GMOS afterglow spectroscopy (which determined the redshift), they also obtained two ground-based (again, Gemini/GMOS and VLT/X-shooter, at 11 and 20 days post-burst, respectively) and two space-based (HST WFC3 grism, at 11 and 35 days) spectra, at the beginning and during the SN. Curiously, while confirming the reddening seen in the photometry, these spectra do not show clear undulations which would be expected from a typical Type Ic-BL SN associated with a GRB (L14; G15). On the other hand, while redder in comparison to the early afterglow, these spectra were much bluer in the rest-frame UV than expected for a typical GRB-SN. We note there is another possible SN which shows a similar rather blue and flat spectral energy distribution (SED), namely the late-time bump associated with XRF 030723, although a spectroscopic redshift is not even known for this event (see Fynbo et al. 2004; Tominaga et al. 2004 and Huang et al. 2004 for more discussion). We confirm these general results with our own reduction of the X-shooter spectra (Krühler et al. 2015; G15). This leads us to our SN results.

2.2. Highly luminous SN 2011kl

The s values are roughly similar, pointing to an evolution which is somewhat slower than that of SN 1998bw (except for J; in this case, the lack of data during the SN decay may skew the result). However, the k values diverge strongly in colour[2], in an almost monotonic fashion: the bluer, the larger. We find the $i'z'$ k values are identical within errors, the r' k value is significantly larger, and the g' k value even larger than in the case of the r' band. Only the J band, once again, deviates from this pattern. Incidentally, L14 point out that if their late-time J data were to be associated with a SN, it would be superluminous. We also confirm the existence of a flux excess even beyond the extrapolation of the SN spectrum in JH from our reduction of the X-shooter spectrum at 19.8 days (see the Extended Data in G15).

This is in full agreement with our second result: the SN is very luminous in general, especially after we also correct for the (small) line-of-sight extinction (K18B). In $i'z'$, SN 2011kl is ≈1.8 × SN1998bw in luminosity (0.6 mag brighter), in r' it is 3.1× more luminous (1.2 mag), while it is 5× as luminous in g' (1.75 mag brighter), which is an unprecedented result. We caution that the observed g' band corresponds to the ultraviolet (2735 Å, roughly the UVOT *uvw1* band) in the rest-frame, and there are no data for SN 1998bw in this bandpass, therefore the light curve was derived by extrapolation. The observed r' band (rest-frame wavelength 3700 Å), on the other hand, can be directly compared to the SN 1998bw U-band data, implying that our extrapolation to get an observer-frame g' light curve must be reasonably robust. These values show that SN 2011kl is not just spectrally significantly dissimilar to SN 1998bw because it is much more ultraviolet luminous, but it is also the most luminous GRB-SN detected so far (G15, Sect. 4.1).

A conservative estimate of the minimum luminosity of the SN can be gained by fitting the afterglow with an unbroken power-law, increasing the afterglow contribution to the total optical transient at the time of the SN. This yields a significantly worse fit of $\chi^2 = 183.7$ for 111 degrees of freedom for the simple power-law fit vs. $\chi^2 = 143.5$ for 109 degrees of freedom for the broken power-law fit, yielding $\Delta\chi^2 = 40.2$ for two more degrees of freedom. We find a decay slope identical to α_1 from the broken power-law fit. In addition, once again assuming no SN contribution in the U band, $k_{g'} = 2.51 \pm 0.24$, $k_{r'} = 2.00 \pm 0.14$, $k_{i'} = 1.02 \pm 0.16$, $k_{z'} = 1.05 \pm 0.22$, and $k_J = 2.30 \pm 0.22$, and s values larger than those found from the broken power-law fit in the range 10–20%. These values are significantly less luminous (and unremarkable in $i'z'$), i.e. just 50%–64% of those we find using a broken power-law fit. As stated, however, this fit is significantly worse and can therefore be ruled out in comparison to the broken power-law fit. Such an unbroken power-law would also not be expected (but see Perley et al. 2014; De Pasquale et al. 2016a), and the wide opening angle implied by an extremely late break would increase the energetics of the GRB to a level not accommodated by the magnetar model (but see Metzger et al. 2015), which is strongly supported by the spectral characteristics (G15). Also see Gompertz & Fruchter 2017 for a similar discussion and K18B for a discussion of their results in light of our full data set.

[2] Independent of its actual luminosity, a SN spectrally identical to SN 1998bw would show identical k values independent of the band.

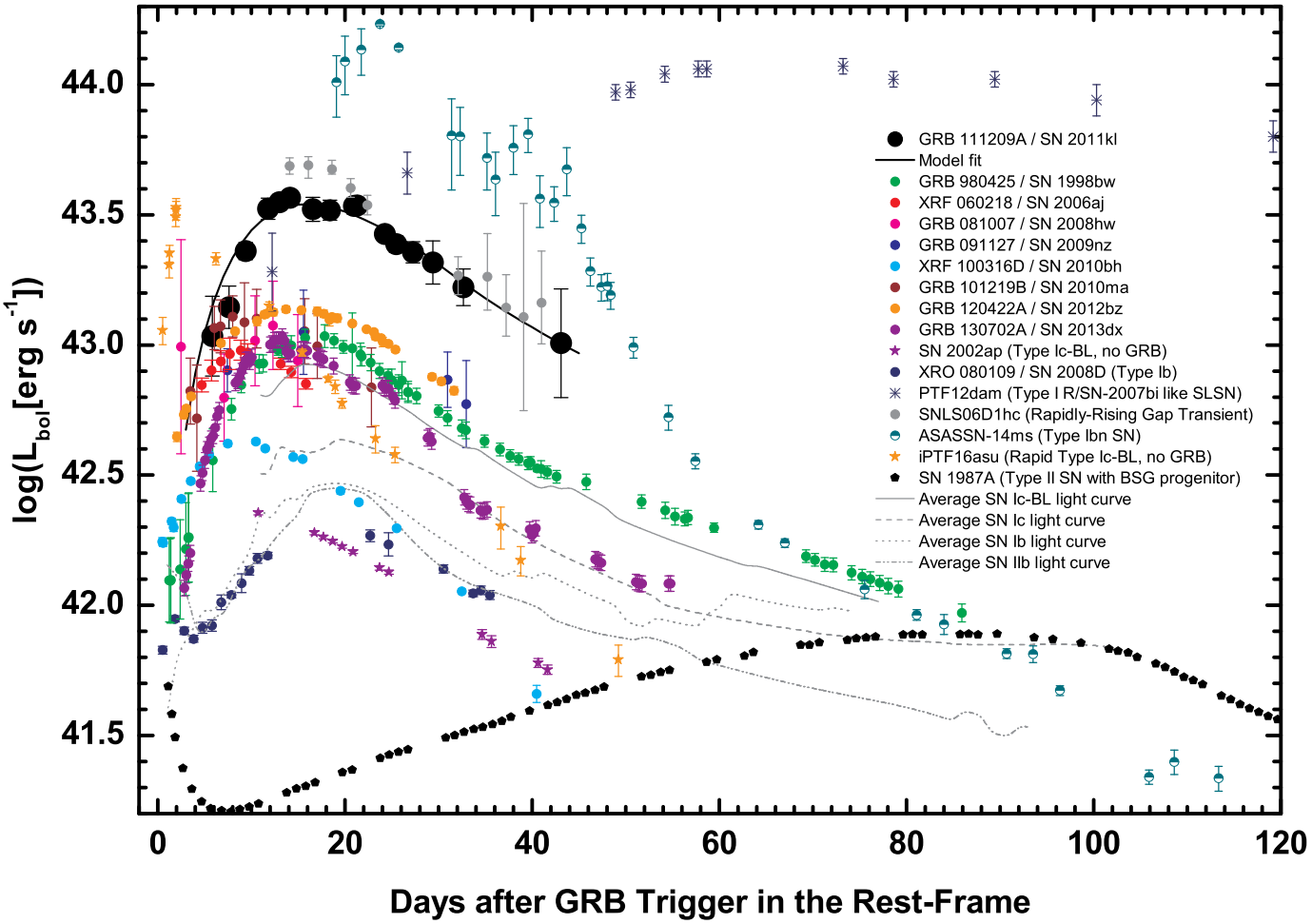

Fig. 2. Bolometric light curves of SE-SNe. SN 2011kl is seen to exceed all other well-monitored GRB-SNe (Olivares et al. 2012, 2015; Prentice et al. 2016) in luminosity, including the bright GRB 120422A/SN 2012bz (Schulze et al. 2014) and the recent well-monitored GRB 130702A/SN 2013dx (Toy et al. 2016). SN 2011kl is far less luminous than SLSNe, exemplified in this figure by PTF12dam (Chen et al. 2015), but of similar luminosity as one of the rapidly rising gap transients (RRGTs) presented by Arcavi et al. (2016); the light-curve evolution is also similar. We assign SNLS06D1hc the same peak time as SN 2011kl. Several further luminous SNe are also shown (see Sect. 4.1.4 for more details). Additionally, we plot mean light curves of four different SE-SNe types taken from Lyman et al. (2016) as well as SN 1987A, which had a BSG progenitor (Suntzeff & Bouchet 1990). We assume $t_{\rm peak}$ = 64 days for PTF12dam (Nicholl et al. 2013; Chen et al. 2015) and $t_{\rm peak}$ = 19 days for the average curves (Lyman et al. 2016).

We initially used the U light curve as a pure afterglow component under the assumption that there would be no contribution from the SN, and now we found that the UV damping usually seen for GRB-SNe does not apply to this object, at least down to approximately the (observer-frame) g' band. Therefore, it is possible that the SN also contributes somewhat to the U-band light curve; in Fig. 1 the data at 16 and 27 days indeed lie marginally above the fit, although this result is not statistically significant. If this is the case, however, our result is only strengthened. Additional SN light in U implies that the intrinsic post-break decay slope must be even steeper, therefore the afterglow contribution during the SN epoch is even smaller, and the SN is even more luminous. Our k results should thus be treated as robust lower limits to the SN luminosity, although we do not expect it to be significantly more luminous than what we have already found.

2.3. Bolometric light curve of SN 2011kl

The bolometric light curve was constructed using the pure SN data from Table 1 in G15 following the methods presented in Olivares et al. (2012, 2015). As not all data are contemporaneous, we used a polynomial of second order for interpolation (and a first-order polynomial at late times) to derive a complete SED at each epoch. We fitted the SEDs using quadratic polynomials (Simpson's rule) and integrated across them (including the observer-frame J-band data). These values were then corrected for a time-dependent rest-frame near-infrared (NIR) contribution based on data of the GRB-SNe SN 1998bw and SN 2006aj (Olivares et al. 2015). The final values represent the bolometric luminosity across the rest-frame 0.3−2.2 μm band.

In Fig. 2, we show the bolometric light curve of SN 2011kl (given in Table 4 and peaking at $L_{\rm bol,peak} = (3.63^{+0.17}_{-0.16}) \times 10^{43}$ erg s^{-1}) in comparison to the bolometric light curves of several other GRB- and XRF-SNe, taken from Olivares et al. (2012, their Fig. 7), Olivares et al. (2015), Schulze et al. (2014), and Toy et al. (2016). We additionally include some non-GRB SE-SNe: the SLSN PTF12dam (Chen et al. 2015), the rapidly-rising gap transient (RRGT) SNLS06D1hc (Arcavi et al. 2016), two more SNe in the luminosity gap between typical GRB-SNe and SLSNe (Vallely et al. 2018; Whitesides et al. 2017), the famous SN 1987A, which had a blue supergiant (BSG) progenitor (Suntzeff & Bouchet 1990), and the mean light curves of

four different SE-SNe types taken from Lyman et al. (2016). We note that in some of these cases, only the observer-frame optical range has been used, implying these are pseudo-bolometric light curves and the true luminosities are higher. This does not change the general picture, however.

Clearly, SN 2011kl is more luminous than any GRB-SN discovered to date; these objects tend to cluster in a relatively narrow luminosity range (Melandri et al. 2014). This includes the previous record holder, SN 2012bz, associated with GRB 120422A (Schulze et al. 2014), and generally the most luminous Type Ic SN which is not a bona fide SLSN (Prentice et al. 2016). It is also much more luminous and evolves much faster than the BSG-progenitor SN 1987A. On the other hand, it is much less luminous and also much faster evolving than PTF12dam. This SLSN shows a light-curve evolution similar to SN 2007bi, which has been claimed to be due to a very massive star exploding as a pair-instability supernova (PISN; Gal-Yam et al. 2009). Such SLSNe were labelled "SLSN R" by Gal-Yam (2012), but Nicholl et al. (2013) and Chen et al. (2015) showed that other similar SNe, including PTF12dam, can also be powered by magnetars (or possibly black holes, BHs; Nicholl et al. 2015a) or the interaction of the SN ejecta with a massive shell ejected at an earlier time; the latter model needs a lot of fine-tuning, however. Therefore these SLSNe are now labelled "2007bi-like". Nicholl et al. (2017a) and De Cia et al. (2018) found a continuum of rise/decay times from large samples with no evidence for any bimodality. Our main motivation in using this specific SLSN as a comparison in Fig. 2 is that the pseudo-bolometric light curve was freely available. See G15 for a comparison to two faster SLSNe.

Furthermore, we show a fit to the 0.3−2.2 μm bolometric light curve using a two-component ^{56}Ni decay model that has a high-density inner region, which is of high opacity and only dominates in the nebular phase, and a low-density outer region which dominates the early SN emission (based on Arnett 1982 and Maeda et al. 2003). As the expansion velocity of the SN could not be determined from spectroscopy because of the lack of any kind of readily detectable absorption lines (L14; G15; Mazzali et al. 2016), the model assumes a typical (for a Type Ic-BL SN) expansion velocity at peak, namely $v_{\rm exp} = (21 \pm 7) \times 10^4\,{\rm km\,s^{-1}}$; this value is close to that used by G15 and Mazzali et al. (2016) for modelling as well. We use a grey opacity of $0.07 \pm 0.01\,{\rm cm^2\,g^{-1}}$ that is identical to Olivares et al. (2015) and G15. The deduced values of the nickel mass created in the explosion $M_{\rm Ni}$, ejecta mass $M_{\rm ej}$, total kinetic energy in the ejecta $E_{\rm k}$, and mass and energy fractions of the inner component of the two-component model are given in Table 3. The span of $M_{\rm ej}$ (3.95−10.46 $M_\odot$) and $E_{\rm k}$ ([2.26−68.33] $\times 10^{51}$ erg) are large because of the large error in velocity, but we note that the derived nickel mass $M_{\rm Ni} = 2.27 \pm 0.64\,M_\odot$ is independent of $v_{\rm exp}$.

The G15 authors do not use the J-band data or a NIR correction, and therefore derive lower values of $L_{\rm bol,peak} = (2.8^{+1.2}_{-1.0}) \times 10^{43}\,{\rm erg\,s^{-1}}$, $M_{\rm ej} = 3.2 \pm 0.5\,M_\odot$, and $M_{\rm Ni} = 1.0 \pm 0.1\,M_\odot$. Cano et al. (2016), using values from G15, derived $M_{\rm ej} \approx 5.2\,M_\odot$, which is in better agreement with our value. Metzger et al. (2015) assumed that beyond the magnetar heating, a typical amount of nickel is also present ($M_{\rm Ni} \approx 0.2\,M_\odot$) and they found that $M_{\rm ej} \approx 3\,M_\odot$, which agrees well with G15, although the former work used a grey opacity of $0.2\,{\rm cm^2\,g^{-1}}$. Bersten et al. (2016) also modelled the bolometric data of G15 with their own magnetar model, which uses $M_{\rm Ni} = 0.2\,M_\odot$ and $M_{\rm ej} = 2.5\,M_\odot$, and they also employed a grey opacity of $0.2\,{\rm cm^2\,g^{-1}}$. They found a best fit when at least some of the SN heating is due to radioactive decay ($M_{\rm Ni} \geq 0.08\,M_\odot$). Yu et al. (2017) derived a significantly smaller $M_{\rm ej} = 0.51 \pm 0.06\,M_\odot$. Finally, Wang et al. (2017a) modelled the bolometric light curve presented in this paper and found it can also be fit by a pure magnetar model or a magnetar+^{56}Ni model. Using $\kappa = 0.07\,{\rm cm^2\,g^{-1}}$, as we do (see also G15), they derive $M_{\rm ej} = 4.50^{+1.76}_{-1.16}\,M_\odot$, $M_{\rm Ni} = 0.11^{+0.06}_{-0.07}\,M_\odot$. Their pure ^{56}Ni model (again, for $\kappa = 0.07\,{\rm cm^2\,g^{-1}}$) results in $M_{\rm ej} = 4.57^{+0.80}_{-1.03}\,M_\odot$, $M_{\rm Ni} = 1.42 \pm 0.04\,M_\odot$, which is somewhat lower than our values, but in full agreement with the conclusions of G15 and our work that a pure ^{56}Ni model is untenable. As a side note, we point out that using our maximum bolometric luminosity $\log L_{\rm peak} = 43.56$ and Eq. (2) from Kozyreva et al. (2016), we derive $M_{\rm Ni} = 5.6\,M_\odot$, an even more extreme value. We discuss these results in the context of larger SN samples in Sect. 4.1.

3. Results

3.1. Blackbody fit of the pure supernova

Using the afterglow fit derived in Sect. 2.1 and the host galaxy magnitudes, we subtract the individual contributions of afterglow and host for each band, leaving the pure magnitudes of the SN. We then also correct these values for the rest-frame extinction derived by K18B. These values are given as Table 1 in G15. Employing our selected cosmology, the redshift $z = 0.67702$, and including a correction for the local velocity field (Mould et al. 2000), we derive a luminosity distance of 4076.5 Mpc, which translates into a distance modulus of $\mu = 43.05$ mag. This allows us to translate the tabulated values from G15 into rest-frame time and absolute magnitudes at the rest-frame wavelengths given in Table 1. We give the derived values in Table 2.

We fitted the flux densities of the SN component using the `zbbody` tool part of the `Xspec v12.7.1` software package[3], assuming that it can be modelled by blackbody radiation. The quality of our optical photometry ($g'r'i'z'$) is best for the epochs at 1.88, 2.40, 3.09, and 3.69 Ms/21.77, 27.79, 35.78, and 42.70 days (Table 2). The J-band is not included as the flux excess places it above the blackbody fit. In this time span the blackbody temperature $T_{\rm bb}$ (in the host frame) decreased from $9.98^{+0.81}_{-0.70}$ kK to 8.70 ± 0.35 kK. At the same time, the bolometric luminosity $L_{\rm bb}$ dropped from $3.3 \times$ to $1.8 \times 10^{43}\,{\rm erg\,s^{-1}}$, while the radius of the emitting shell, defined via $R_{\rm bb} = (L_{\rm bb}/4\pi\sigma T_{\rm bb}^4)^{1/2}$ was about 2.3×10^{15} cm (see Fig. 3, and Table 5).

3.2. Absolute magnitudes for SN 2011kl

Using data from Clocchiatti et al. (2011) and McKenzie & Schaefer (1999), and correcting for the small Galactic line-of-sight extinction (Schlafly & Finkbeiner 2011), we employ the analytical equation derived by Zeh et al. (2004) to derive the maximum brightness of SN 1998bw in the U, B, V, and R_C bands independent of data scatter and sampling density, finding (Vega magnitudes) $U = 13.891$ mag, $B = 14.146$ mag, $V = 13.673$ mag, and $R_C = 13.598$ mag; these values are not yet corrected for host-galaxy extinction. Using the precise host-galaxy redshift of $z = 0.00867$ (Foley et al. 2006), we derive a luminosity distance of $D_{\rm L} = 35.5$ Mpc to SN 1998bw via CosmoCalc[4] (Wright 2006), our assumed world model, and the

[3] http://heasarc.nasa.gov/xanadu/xspec/
[4] http://www.astro.ucla.edu/~wright/CosmoCalc.html

Table 2. The values from Table 1 in G15, given in the rest-frame.

$\Delta t_{\rm obs}$ (s)	$\Delta t_{\rm obs}$ (d)	$\Delta t_{\rm rest}$ (s)	$\Delta t_{\rm rest}$ (d)	M_{2735} mag	M_{3709} mag	M_{4556} mag	M_{5360} mag	M_{7394} mag
843 664	9.7646	503 073	5.8226	$-18.69^{+0.26}_{-0.21}$	$-19.13^{+0.23}_{-0.19}$	$-19.02^{+0.55}_{-0.38}$	$-19.08^{+1.13}_{-0.57}$	...
1 101 930	12.7538	657 076	7.6050	$-18.88^{+0.29}_{-0.24}$	$-19.39^{+0.16}_{-0.14}$	$-19.25^{+0.44}_{-0.33}$	$-19.22^{+0.75}_{-0.48}$	...
1 358 649	15.7251	810 157	9.3768	...	...	...	...	-20.67 ± 0.09
1 360 463	15.7461	811 238	9.3893	...	...	$-19.77^{+0.12}_{-0.11}$	...	...
1 361 742	15.7609	812 001	9.3982	...	...	...	$-19.89^{+0.28}_{-0.25}$	...
1 705 078	19.7347	1 016 731	11.7677	-19.46 ± 0.04	...	...	...	...
1 706 253	19.7483	1 017 432	11.7758	...	-20.06 ± 0.04	...	...	...
1 880 549	21.7656	1 121 363	12.9787	-19.58 ± 0.15	-20.15 ± 0.07	-20.31 ± 0.13	$-20.27^{+0.19}_{-0.18}$	$-20.87^{+0.39}_{-0.35}$
2 049 952	23.7263	1 222 378	14.1479	...	...	...	...	-20.75 ± 0.06
2 401 323	27.7931	1 431 899	16.5729	$-19.52^{+0.28}_{-0.27}$	-19.80 ± 0.15	-20.15 ± 0.17	$-20.38^{+0.23}_{-0.22}$	$-20.51^{+0.53}_{-0.48}$
2 664 187	30.8355	1 588 644	18.3871	...	...	...	...	$-20.43^{+0.16}_{-0.15}$
3 037 306	35.1540	1 811 133	20.9622	...	...	...	...	$-20.47^{+0.22}_{-0.21}$
3 085 966	35.7172	1 840 149	21.2980	...	...	...	...	-20.64 ± 0.07
3 090 966	35.7751	1 843 130	21.3325	$-19.17^{+0.18}_{-0.17}$	-19.84 ± 0.11	$-20.00^{+0.17}_{-0.16}$	-20.35 ± 0.19	...
3 518 554	40.7240	2 098 099	24.2836	...	...	...	...	-20.24 ± 0.09
3 692 304	42.7350	2 201 705	25.4827	...	...	-19.70 ± 0.12	...	...
3 693 574	42.7497	2 202 463	25.4915	...	...	...	$-19.84^{+0.23}_{-0.22}$	...
3 694 905	42.7651	2 203 256	25.5007	-18.69 ± 0.07	...	...	...	...
3 696 071	42.7786	2 203 952	25.5087	...	-19.45 ± 0.05	...	...	...
3 950 847	45.7274	2 355 874	27.2671	...	...	...	...	-20.24 ± 0.09
4 258 444	49.2875	2 539 292	29.3900	$-18.64^{+0.39}_{-0.37}$	-19.25 ± 0.20	$-19.42^{+0.42}_{-0.40}$	$-19.61^{+0.62}_{-0.58}$	...
4 732 196	54.7708	2 821 789	32.6596	$-18.36^{+0.63}_{-0.58}$	$-18.77^{+0.27}_{-0.26}$	$-19.25^{+0.32}_{-0.31}$	$-19.38^{+0.48}_{-0.46}$	...
6 241 880	72.2440	3 722 007	43.0788	...	$-17.79^{+0.84}_{-0.74}$	$-18.76^{+0.78}_{-0.73}$	$-18.78^{+1.57}_{-1.34}$	...

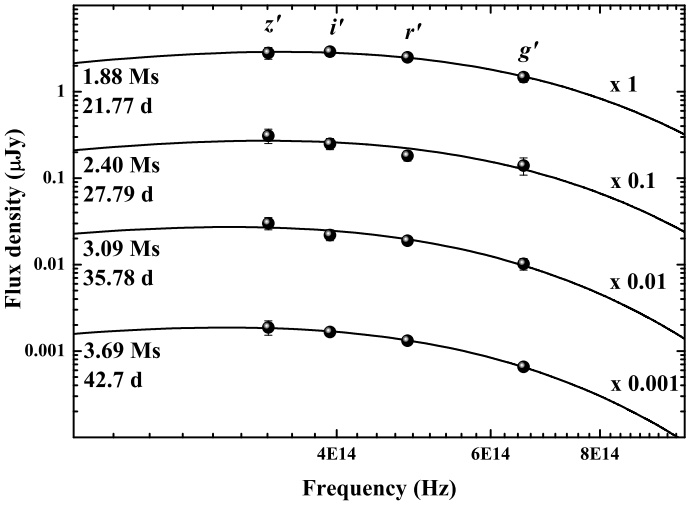

Fig. 3. Blackbody fits to the GROND $g'r'i'z'$-band data of SN 2011kl (times in observer frame, Table 2). We note that for reasons of clarity the y-axis was scaled by the given factors.

NED Velocity Correction Calculator[5]. From this, we derive a distance modulus of 32.75 mag, and thus $M_U = -19.17$ mag, $M_B = -18.87$ mag, $M_V = -19.28$ mag, and $M_{R_C} = -19.31$ mag for SN 1998bw. We assume a host-galaxy extinction for SN 1998bw of $A_V = 0.2$ mag (Woosley et al. 1999), which is the same value used to derive the template light curves for all our GRB-SN fits. This value is fully in agreement with the result derived at the SN location by Krühler et al. (2017).

[5] http://ned.ipac.caltech.edu/forms/vel_correction.html

At the redshift of GRB 111209A/SN 2011kl, the observed filters do not correspond to the rest-frame $UBVR_C$ filters, although $U_{\rm rest}$ is essentially the same as r', i' lies just slightly redwards of $B_{\rm rest}$, and z' lies slightly bluewards of $V_{\rm rest}$, in terms of central wavelengths. Only $R_{C,\rm rest}$ lies roughly in the middle between z' and J, corresponding to Y. We find that the five k values we derive, if plotted over the observer-frame central wavelengths of the filters, can be well interpolated ($\chi^2 = 0.89$ for 2 degrees of freedom) with a polynomial of second order. From this fit, we derive $k_{U,\rm rest} = 3.09 \pm 0.16$, $k_{B,\rm rest} = 2.05 \pm 0.13$, $k_{V,\rm rest} = 1.62 \pm 0.15$, and $k_{R_C,\rm rest} = 2.33 \pm 0.18$, leading to $M_U = -20.39 \pm 0.06$ mag, $M_B = -19.65 \pm 0.07$ mag, $M_V = -19.80 \pm 0.10$ mag, and $M_{R_C} = -20.23 \pm 0.09$ mag. We note that this fit ignores the spectral dissimilarities between SN 1998bw and SN 2011kl (G15), but as mentioned most rest-frame central wavelengths lie close to observer-frame bands.

4. Discussion

4.1. Supernova associated with GRB 111209A in context

The excellent agreement with the temporal evolution of SN 1998bw (Sect. 2.1) gives us high confidence that we are indeed seeing a SN following GRB 111209A, which is significantly more luminous than the prototypical SN 1998bw itself. Indeed, SN 2011kl is the most luminous GRB-SN (with a high-confidence detection) found so far. This conclusion is fully borne out by the spectroscopic classification of the SN (G15). Relativistic tidal disruption flares (Levan et al. 2011; Cenko et al. 2012; Brown et al. 2015) are not expected to be accompanied by any kind of significantly brightening late-time emission which would look similar to a SN. This is a further indicator that GRB 111209A is an extreme case of a classical GRB.

Table 3. Results of modelling the SN with a two-component ^{56}Ni decay model.

Expansion velocity $v_{\rm exp}$ (10^3 km s^{-1})	21 ± 7
Ejected mass $M_{\rm ej}$ ($M_\odot$)	$6.79^{+3.67}_{-2.84}$
Ejecta kinetic energy $E_{\rm k}$ (10^{51} erg)	$34.26^{+34.07}_{-32.00}$
Nickel mass $M_{\rm Ni}$ ($M_\odot$)	2.27 ± 0.64
Mass fraction, inner component	0.31 ± 0.19
Energy fraction, inner component	0.000 ± 0.003

Notes. The expansion velocity is an input parameter.

Table 4. The bolometric light curve of GRB-SN 111209A, given in the rest-frame.

Δt (ks)	Bolometric peak luminosity (log($L_{\rm bol}$)(ergs^{-1}))
503	43.03 ± 0.15
657	43.14 ± 0.08
811	43.36 ± 0.03
1017	43.52 ± 0.04
1122	43.55 ± 0.03
1223	43.56 ± 0.02
1432	43.52 ± 0.05
1589	43.52 ± 0.04
1811	43.53 ± 0.03
1842	43.54 ± 0.03
2098	43.43 ± 0.02
2203	43.39 ± 0.03
2356	43.36 ± 0.04
2539	43.32 ± 0.08
2822	43.22 ± 0.07
3722	43.01 ± 0.21

While there is strong evidence that SN 2011kl is not fully powered by radioactive decay (G15; Metzger et al. 2015; Bersten et al. 2016; Cano et al. 2016; Yu et al. 2017; Wang et al. 2017a), we for now continue with the results from the ^{56}Ni modelling to show just how much of an outlier SN 2011kl is in such a context.

To allow a direct comparison of SN 2011kl and other GRB-SNe, we also undertake systematic multi-colour afterglow/SN analysis of a large sample of GRB-SNe (Kann et al., in prep.). The main conclusion of this analysis is twofold: several of the multi-colour GRB-SNe show divergences from SN 1998bw spectrally (e.g. SNe 2010bh and 2012bz), and none exceed SN 2011kl in luminosity. The exceptional ultraviolet luminosity of SN 2011kl therefore seems unique, at least in comparison to the currently known sample.

4.1.1. SN 2011kl and SLSNe

In recent years, a special class of ultra-luminous, UV-bright (e.g. Tolstov et al. 2017) transients has been recognized by Quimby et al. (2011, see Gal-Yam 2012 and Moriya et al. 2018; Gal-Yam 2018 for reviews). Pastorello et al. (2010) presented more detailed observations of one of the Quimby et al. (2011) sources and linked these to Type Ic SNe, thereby implying that UV suppression is not a given for such SE-SNe, at least not around peak time (see also Inserra et al. 2013). Indeed, nebular spectroscopy of several events reveals that at very late times, they are spectroscopically indistinguishable from SNe associated with GRBs (Nicholl et al. 2016a; Jerkstrand et al. 2017; Kangas et al. 2017; Quimby et al. 2018). The classical, albeit arbitrary definition of SLSNe is $M_U < -21$ at peak, therefore SN 2011kl is not a SLSN per se. Recently, though, the designation has been applied to other luminous SNe that fall under the luminosity limit but are spectrally clearly similar to SLSNe (e.g. De Cia et al. 2018; Lunnan et al. 2018a; Quimby et al. 2018; Angus et al. 2018) leading other authors to designate SN 2011kl as a SLSN (e.g. Liu et al. 2017b; Margutti et al. 2018).

Within the statistical four observables parameter space (4OPS) context (see Inserra et al. 2018a, for details), we find that SN 2011kl is not fully but mostly in agreement with the parameter space of SLSNe; this contrasts to what Inserra et al. (2018a) have found for GRB-SNe. We note, however, that Angus et al. (2018) have also presented multiple spectroscopically classified SLSNe that do not agree with all four panels. It is therefore unclear how strong a diagnostic tool this is at this stage.

It has been found that these SLSNe are also found in dwarf host galaxies which seemed to resemble those of GRBs (Chen et al. 2013; Lunnan et al. 2013, 2014), but have been shown to have even more extreme properties (e.g. Leloudas et al. 2015a; Thöne et al. 2015; Perley et al. 2016; Schulze et al. 2018). The single exception may be the host of the closest SLSN, SN 2017egm, which is a large spiral galaxy for which an approximately solar or even super-solar metallicity is claimed (Nicholl et al. 2017c; Bose et al. 2018; Chen et al. 2017a; Yan et al. 2018), but see Izzo et al. (2018) concerning metallicity diagnostics; these authors have found $Z = 0.6\,Z_\odot$ just above the possible metallicity cut-off (e.g. Schulze et al. 2018). Indeed, SLSNe may be the very first SNe to occur in the youngest starbursts, even earlier than GRBs (Leloudas et al. 2015a; Thöne et al. 2015). Similar to GRBs, they can be detected to very high redshifts, ranging from $z \approx 1-4$ (Cooke et al. 2012; Moriya et al. 2019; Curtin et al. 2019; Angus et al. 2018). While Moriya et al. (2010) suggested it may be possible, none of these events have been associated with GRBs or relativistic blast waves in general (Coppejans et al. 2018). Sanders et al. (2012) specifically looked for a connection in the case of SN 2010ay, which strongly resembles GRB-SNe, but, with the exception of that event, these transients are spectroscopically very different from GRB-SNe. In contrast to GRBs and their afterglows/SNe, they have also not yet been detected at very high energies (Renault-Tinacci et al. 2018), in gamma-rays, X-rays (Margutti et al. 2018; Bhirombhakdi et al. 2018, with a few exceptions, Levan et al. 2013; Margutti et al. 2018), or at radio wavelengths (Coppejans et al. 2018).

Even though it is comparatively UV luminous, SN 2011kl does not exhibit such high blackbody temperatures as are found for these SLSNe around maximum, which are typically in the range 14−17 kK (e.g. Quimby et al. 2013). Some SLSNe have lower temperatures at peak which are more comparable to that of SN 2011kl, and even lower values at peak have been measured, for example 7 kK for iPTF13ehe (Yan et al. 2015). SN 2011kl is hotter than usual Type Ic-BL SNe, however; several GRB-SNe shown in Nicholl et al. (2015b, their Fig. 18) show temperatures at peak of 6−8 kK.

In terms of luminosity, SN 2011kl falls below the luminosities of most SLSNe. A direct comparison free of any bolometric transformations can be done vs. the SLSN DES13S2cmm, which lies at almost exactly the same redshift (Papadopoulos et al. 2015); this SLSN is about 0.9 mag brighter at peak than SN 2011kl. The largest $L_{\rm bb}$ we measure is $(3.67 \pm 0.21) \times 10^{43}$ erg s^{-1}, while SLSNe may reach up to $>200 \times 10^{43}$ erg s^{-1} (ASASSN-15lh; Dong et al. 2016; Godoy-Rivera et al. 2017; Brown et al. 2016, but see Leloudas et al. 2016; Margutti et al. 2017;

Table 5. Results of the blackbody fits.

Δt (Ms/d)	$T_{\rm bb}$ (kK)	χ^2_ν	$L_{\rm bb}$ (10^{43} erg s^{-1})	$R_{\rm bb}$ (10^{15} cm)
1.88/21.77	$9.98^{+0.81}_{-0.70}$	0.04	3.27 ± 0.17	2.1 ± 0.4
2.40/27.79	9.17 ± 1.28	0.94	2.68 ± 0.24	2.3 ± 0.6
3.09/35.78	$8.94^{+0.81}_{-0.70}$	0.57	2.57 ± 0.20	2.4 ± 0.5
3.69/42.70	8.70 ± 0.35	0.04	1.80 ± 0.09	2.1 ± 0.2

Krühler et al. 2018, who present strong evidence that this is actually a tidal disruption event). Figure 4 shows[6], in contrast, that not only is SN 2011kl more luminous at peak than all known GRB-SNe; this object is also is comparable to the least luminous of the SNe that have been labelled superluminous, at least pseudo-bolometrically. We caution here that while all GRB-SNe shown except for SN 2016jca (Ashall et al. 2017; Cano et al. 2017b), iPTF17cw (Corsi et al. 2017), SN 2017htp (de Ugarte Postigo et al. 2017), and SN 2017iuk (Izzo et al. 2019) have had their bolometric luminosities determined with the same method (Olivares et al. 2015), the bolometric luminosities of the SLSNe and other transients are usually based on observer-frame optical data only (pseudo-bolometric) and therefore their true bolometric luminosities may be higher.

It should be briefly mentioned that pair-instability SNe (Barkat et al. 1967; Fraley 1968), which have been posited as viable SLSN progenitors (e.g. Gal-Yam et al. 2009; Cooke et al. 2012, but see e.g. Nicholl et al. 2013), are very unlikely to be linked to GRBs, even ULGRBs; this is because they disrupt the star entirely, leaving no compact remnant. Furthermore, the host galaxy of GRB 111209A is also likely too metal-enriched to host such super-massive stars (L14; Stratta et al. 2013; despite having a low metallicity within the ensemble of GRB host galaxies; Krühler et al. 2015). On the other hand, the magnetar model which we favour for SN 2011kl (G15) has been found to be able to fit SLSNe well, both photometrically and spectroscopically (e.g. Nicholl et al. 2013, 2017a; Mazzali et al. 2016).

Nicholl et al. (2015b) studied a moderately large sample of SLSNe. They derived rise and decline times for the pseudo-bolometric light curves, defined as the time between when the luminosity is at $L_{\rm peak}/e$ to $t_{\rm peak}$, and from then to when it has declined again to $L_{\rm peak}/e$. We follow their method and fit our bolometric light curve with a fourth-order polynomial, finding $t_{\rm peak} = 16.1$ days in the rest-frame, $\log L_{\rm peak} = 43.58$, and rise and decline times of 9.1 and 21.1 days, respectively, from this fit. This implies the light curve is narrower than those of all SLSNe in the sample of Nicholl et al. (2015b), not just the SLSN-2007bi-like SLSNe as stated above (see also G15). We also compared SN 2011kl with the (i)PTF sample recently presented by De Cia et al. (2018), who, instead of using e, derived rise and decline times for 1 mag and a factor 2. For these values, we find rise times of 8.8 and 7.8 days and decline times of 19.2 and 14.4 days, respectively. Only PTF 09as (11/9 days) and PTF 10aagc (14/10 days) decline faster, and iPTF13bjz rises comparably fast (9/8 days). Interestingly, the two former SLSNe are among the least luminous in their sample, comparable to or even fainter than SN 2011kl. iPTF 13bzj is more luminous, but still lies beneath the classic SLSN luminosity cut-off, and is sparsely sampled.

SN 2011kl agrees well with the full-sample correlation of Nicholl et al. (2015b; their Fig. 4), but also does not deviate significantly from the Type Ibc SNe in this plot. Furthermore,

[6] See appendix for the data sources.

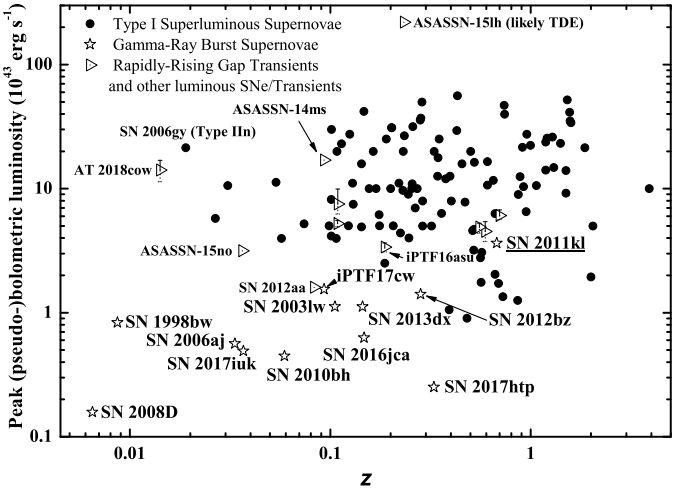

Fig. 4. Comparison between the bolometric luminosity at peak of GRB-SNe, SLSNe, the RRGTs (Arcavi et al. 2016) and other luminous SNe (see Sect. 4.1.4 for more details). SN 2011kl is more luminous than any GRB-SN known and is comparable to the least luminous SLSNe (being possibly even more luminous than a few) and the RRGTs. While most of the GRB-SNe have bolometric luminosities that include a NIR correction (Olivares et al. 2012, 2015), this is not the case for all SLSNe or the RRGTs. Therefore, in some cases, the bolometric luminosities may be underestimated. Furthermore, SN 2008D, a Type Ib SN, is not associated with relativistic ejecta (Soderberg et al. 2008; Malesani et al. 2009) and therefore strictly not a GRB-SN, but a possible transition object.

Nicholl et al. (2015b) discussed whether, in luminosity space, there are two distinct populations of Type Ic SNe (normal + BL vs. SLSNe) or whether there is a continuum. Indeed, SN 2011kl is a transition object indicating that a continuum indeed exists (similar to what has been found for hydrogen-rich SLSNe; Inserra et al. 2018b); see also G15 and the discussion below (Sect. 4.1.4).

In the context of the magnetar model, Yu et al. (2017) have studied a large sample of SLSNe bolometric light curves; these authors include SN 2011kl within this sample. Within the spread of values they derived, SN 2011kl is seen as an outlier. The least luminous SLSN in the sample, this object has the lowest ejecta mass (smaller by an order of magnitude compared to our ^{56}Ni modelling), longest initial magnetar spin period, lowest rotational energy, one of the lowest spin-down luminosities, and one of the strongest magnetic fields. Liu et al. (2017a) also modelled SLSNe (but not SN 2011kl) with a magnetar model and all their SLSNe have more rapidly spinning magnetars and larger ejecta masses than SN 2011kl as derived by Yu et al. (2017). The SN 2011kl light curve also shows one of the fastest rise times. Only the light-curve decay time and the spin-down timescale of the magnetar are found to be average values within the distributions. But in the correlations that Yu et al. (2017) studied, SN 2011kl was found to be at the extreme end in several cases; while still agreeing with the trends, it is not an outlier. They also compared their SLSN sample with values derived for GRB-SNe by Lü & Zhang (2014), for which caution must be exercised as the magnetars in their modelling also power the GRB prompt and afterglow emission, and not just the SNe. Thus in terms of magnetar field strength, SN 2011kl lies at the boundary between SLSNe (low field strengths) and GRB-SNe (high field strengths) and is once more a transition object, but it is not unique in this aspect. These authors note that the magnetic field strength is strong enough to launch a jet, but it is near the critical

field strength; for GRB-SNe, the field is always strong enough and for SLSNe, the field in most cases is not strong enough.

4.1.2. SN 2011kl and SE-SNe

To put SN 2011kl into a larger context of more similar SNe, we look into the literature for large comparison samples of SE-SNe (Types IIb, Ib, Ic, BL-Ic, GRB-SN). Cano (2013) used a bolometric approximation method to derive bolometric properties for GRB/XRF SNe and non-GRB-related Type Ibc SNe, some of which are BL. In an older paper (Cano et al. 2011), they also presented a sample of absolute magnitudes M_V for Type Ibc SNe. Cano et al. (2017a) derived improved average GRB-SN values based on updated data. Richardson et al. (2014) studied large samples of all types of SNe (including non-SE SNe and Type Ia SNe) and derived median absolute M_B magnitudes for the various samples. They found $\overline{M_B} = -16.99 \pm 0.45$ mag, $\overline{M_B} = -17.45 \pm 0.33$ mag, and $\overline{M_B} = -17.66 \pm 0.40$ mag for Type IIb, Type Ib, and Type Ic SNe, respectively; these values are far fainter than the value we find for SN 2011kl. Lyman et al. (2016) derived bolometric light curves for 38 SE-SNe and used these to determine explosion parameters; this sample partially overlaps with that of Cano (2013). Finally, Walker et al. (2014) compiled a literature sample of explosion parameters for Type Ic-BL SNe and presented their analysis of PTF10qts. We take four Type Ic-BL SNe from this paper which are not found in the other samples.

Cano (2013) found that in terms of $M_{\rm Ni}$, $M_{\rm ej}$, and $E_{\rm k}$, the SNe associated with GRBs and XRFs yield significantly higher values than those derived for typical Type Ib/c SNe, and even for Type Ic-BL SNe not associated with GRBs/XRFs. For GRB/XRF SNe, the median values they derived are $\overline{M_{\rm Ni}} = 0.3{-}0.35\,M_\odot$, $\overline{M_{\rm ej}} = 6.0\,M_\odot$, and $\overline{E_{\rm k}} = 20 \times 10^{51}$ erg. The values we derive for SN 2011kl (Sect. 2.3 and Table 3) are comparable in terms of $M_{\rm ej}$, for the most part higher in terms of $E_{\rm k}$, and significantly higher in terms of $M_{\rm Ni}$; indeed, Lyman et al. (2016) found that $M_{\rm ej}$ is the one parameter which is distributed evenly among all the SE-SNe classes. This result also remains unchanged in comparison to the average GRB-SN derived by Cano et al. (2017a), who found (excluding SN 2011kl itself) as follows: $\overline{L_{\rm p}} = (1.03 \pm 0.36) \times 10^{43}$ erg s^{-1} (28% of SN 2011kl); $\overline{E_{\rm k}} = (25.2 \pm 17.9) \times 10^{51}$ erg (74% of SN 2011kl, identical within errors); $\overline{M_{\rm ej}} = 5.9 \pm 3.8\,M_\odot$ (87% of SN 2011kl, identical within errors); and $\overline{M_{\rm Ni}} = 0.37 \pm 0.20\,M_\odot$ (16% of SN 2011kl). The two highest ^{56}Ni masses Cano (2013) found for GRB-SNe are both also very uncertain, $M_{\rm Ni} \approx 0.9 \pm 0.5\,M_\odot$ for the SNe accompanying GRBs 991208 and 080319B (see also Cano et al. 2017a). On the opposite end, ^{56}Ni masses can go down to just ≈5% of what we find for SN 2011kl (GRB 060904B, XRF 100316D/SN 2010bh; Olivares et al. 2012, Cano 2013, Cano et al. 2017a). Furthermore, none of the ^{56}Ni masses for any other Type Ibc SN come close to what we find for SN 2011kl. This is also true if the other samples are taken into account. Such a ^{56}Ni mass also far exceeds what could be produced by a magnetar alone (Suwa & Tominaga 2015, Chen et al. 2017c), although Song & Liu (2019) have claimed it can be produced in the outflow for low-metallicity progenitors.

Lyman et al. (2016) presented a large sample of bolometric light curves (their Fig. 1). We find that at peak $M_{\rm bol} = -20.20 \pm 0.05$ mag, using their conversion between peak bolometric luminosity and absolute bolometric magnitude and the peak bolometric luminosity we derive for SN 2011kl ($\log L_{\rm bol} = 43.56$). Using our SN 2011kl values and Eq. (4) of Lyman et al. (2016), we either find $M_{\rm Ni} \approx 1.6\,M_\odot$ by using $M_{\rm bol}$, or we conversely use our modelled value of $M_{\rm Ni}$ to predict $M_{\rm bol} \approx -20.58$ mag. These values are in reasonable agreement with the relation from Lyman et al. (2016). They also derived several different explosion parameters for the events in their sample and plotted these against one another; we follow their methodology and put SN 2011kl into this context, using an expanded sample (Fig. 5) with additional results from sample papers: Cano (2013), Taddia et al. (2018, 2019a), Prentice et al. (2018, only $M_{\rm Ni}$ and $M_{\rm ej}$), as well as several single events as follows: D'Elia et al. (2015, GRB 130702A/SN 2013dx), Toy et al. (2016, GRB 130702A/SN 2013dx), Corsi et al. (2017, iPTF17cw), and Izzo et al. (2019, GRB 171205A/SN 2017iuk). Similar to the averaged-values comparison, we find SN 2011kl to be exceptional in terms of $M_{\rm Ni}$, but ordinary in terms of $M_{\rm ej}$ and $E_{\rm k}$. In the top-most panel, we plot the extremal case $M_{\rm Ni} = M_{\rm ej}$ and $M_{\rm Ni} = M_{\rm ej}/3$, the case for SN 2011kl, and four other SNe, SN 2005hg, SN 2009ca, SN 2010ma, and iPTF17cw. The first two are the most luminous SNe in Lyman et al. (2016) and Taddia et al. (2018), respectively; SN 2010ma is associated with GRB 101219B, while iPTF17cw is an engine-driven Type Ic-BL SN possibly associated with a GRB. This may imply an additional heating source beyond radioactive heating for these SNe as well. We note that SNe exhibiting $M_{\rm ej}/E_{\rm k} = $ const. in the third panel are from Cano (2013) and the seeming correlations stem from their analysis method, i.e. an assumed constant peak photospheric velocity for those SNe that did not have this value spectroscopically measured.

Prentice et al. (2016) presented one of the largest samples of non-SLSN SE-SNe so far, i.e. more than 80, which they analysed consistently. SN 2011kl is the most luminous SN in the sample (see their Figs. 8 and 12). They derived $\log L_{\rm peak} = 43.529^{+0.174}_{-0.148}$ for SN 2011kl (in excellent agreement with our own value), which exceeds the median value they found for the fully bolometric Type Ic-BL/GRB-SNe sample by 0.72 dex. None of their $M_{\rm Ni}$ values exceed $M_{\rm Ni} \approx 0.8\,M_\odot$; they did not derive $M_{\rm Ni}$ for SN 2011kl itself, simply stating that it is magnetar-powered. In addition they found a median for the above-mentioned sample of $M_{\rm Ni} = 0.34^{+0.13}_{-0.19}\,M_\odot$, which is far below our SN 2011kl result. The median values of $\log L_{\rm peak}$ and $M_{\rm Ni}$ for all the other SE-SNe classes (non-BL Ic, Ib, IIb) are yet again lower. We adopt their Figs. 19–21 and show SN 2011kl in comparison to their sample (Fig. 6, we also add the samples of Prentice et al. 2018 (top panel only) and Taddia et al. 2019a). The errors we find for $M_{\rm ej}^3/E_{\rm k}$ for SN 2011kl are large, $M_{\rm ej}^3/E_{\rm k} = 9.15^{+9.6}_{-7.6}$. Clearly, SN 2011kl is a strong outlier. In the top plot of Fig. 6, there is a tight correlation between $\log L_{\rm p}$ and $M_{\rm Ni}$, as expected. SN 2011kl lies beyond all SNe from Prentice et al. (2016, 2018), Taddia et al. (2019a) but is in agreement with the correlation. This correlation implies that the middle and bottom plots contain essentially the same information. The value we derive for $M_{\rm ej}^3/E_{\rm k}$ for SN 2011kl is the second largest in the entire sample, but not extreme. There is a rough trend visible of decreasing $M_{\rm Ni}$ (or $\log L_{\rm p}$) with increasing $M_{\rm ej}^3/E_{\rm k}$, and SN 2011kl lies outside the main cloud similar to two Prentice et al. (2016) events and multiple of the Type Ic-BL SNe studied by Taddia et al. (2019a).

All in all, we find that if we model SN 2011kl as a purely ^{56}Ni-decay powered SN, we find a good fit with a model, but derive results which are physically unrealistic, especially in the context of the spectrum/SED of the SN (see G15; Mazzali et al. 2016, for details). This remains true even in the case of not using the NIR bolometric correction, which leads to a halved ^{56}Ni mass compared to our result (G15).

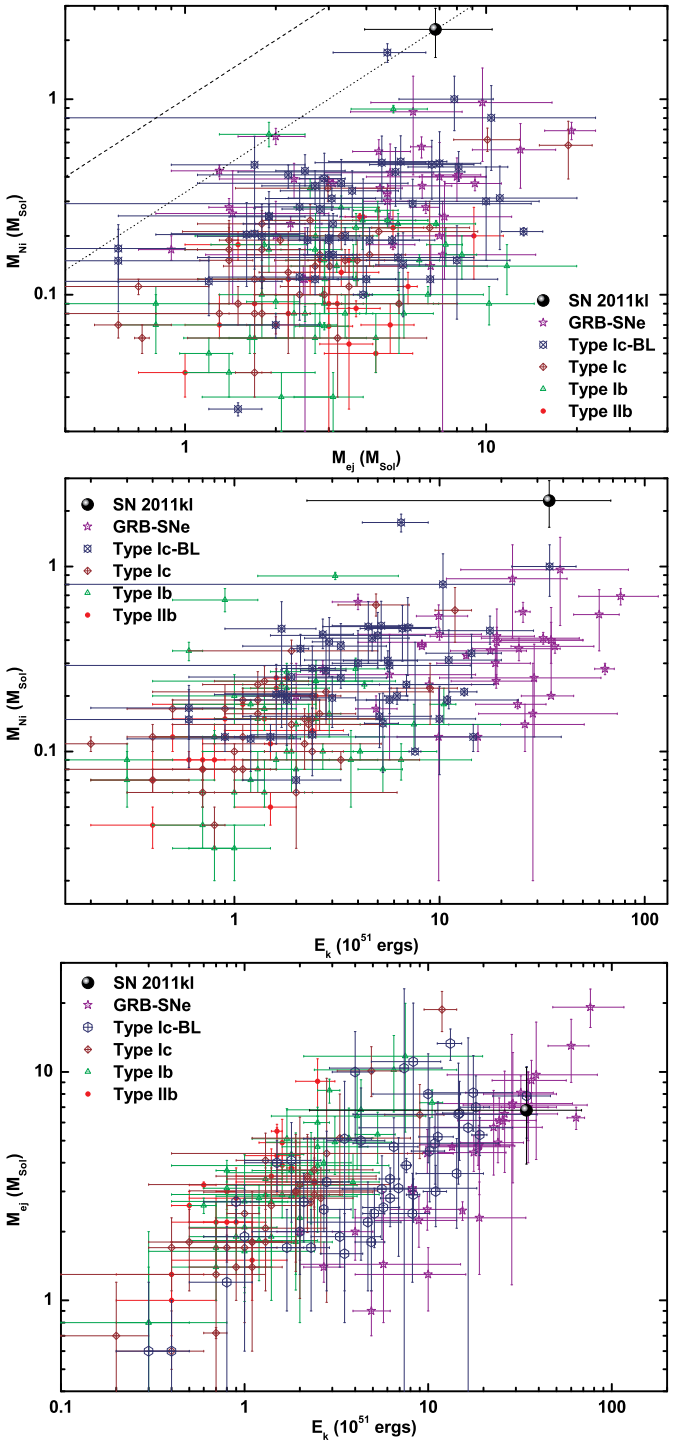

Fig. 5. Explosion parameters of SN 2011kl in the context of SE-SNe following Lyman et al. (2016). *Top panel*: created ^{56}Ni mass $M_{\rm Ni}$ vs. the ejected shell mass $M_{\rm ej}$ (both $M_{\odot}$). SN 2011kl has the highest ^{56}Ni mass of any SN in all the samples, but its ejecta mass is not remarkable. We also plot the extremal case $M_{\rm Ni} = M_{\rm ej}$ (dashed line) and $M_{\rm Ni} = M_{\rm ej}/3$ (dotted line), the case for SN 2011kl. *Middle panel*: $M_{\rm Ni}$ vs. the kinetic energy in the ejecta $E_{\rm k}$ (in 10^{51} erg). SN 2011kl is once again extreme in terms of $M_{\rm Ni}$, but its $E_{\rm k}$ is comparable to most other GRB-SNe. *Bottom panel*: $M_{\rm ej}$ vs. $E_{\rm k}$. SN 2011kl is comparable to the rest of the GRB-SN sample.

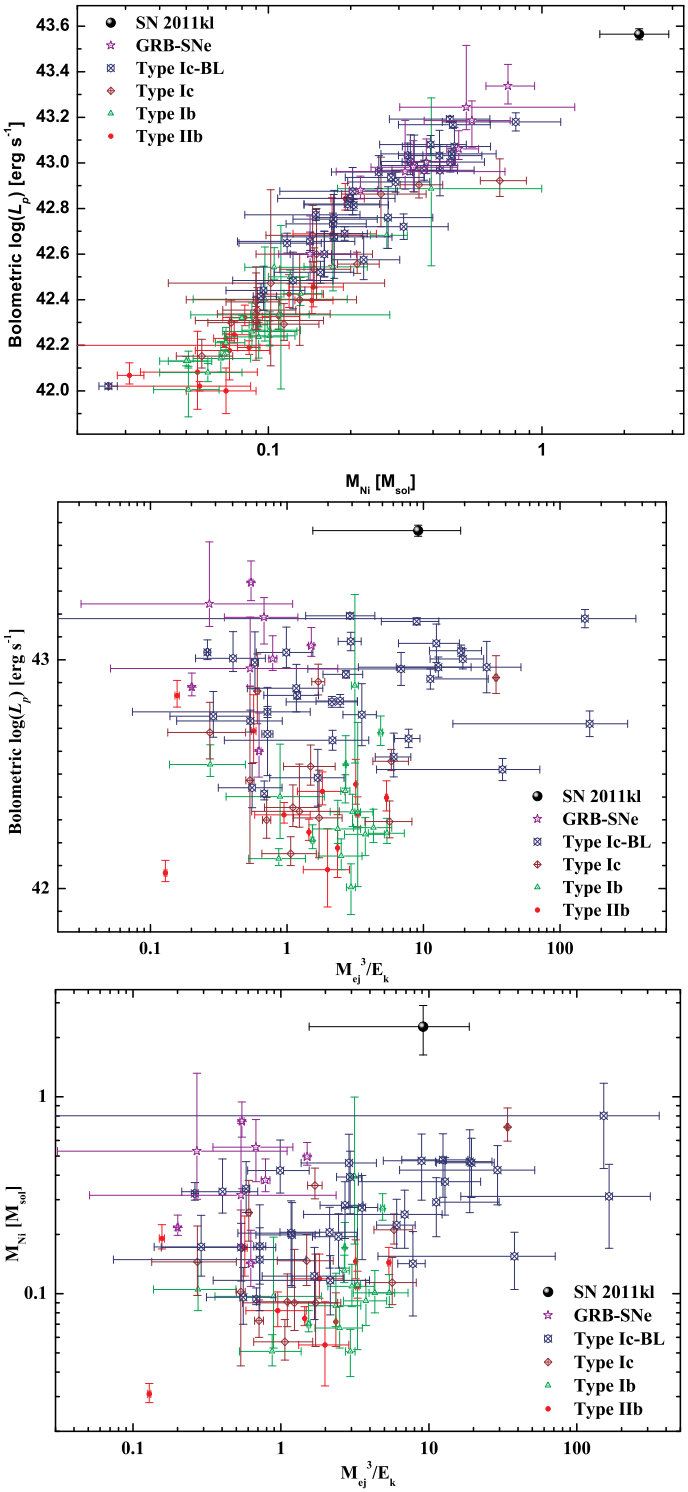

Fig. 6. Explosion parameters of SN 2011kl in the context of SE-SNe following Prentice et al. (2016). *Top panel*: logarithmic bolometric peak luminosity $L_{\rm peak}$ vs. the created ^{56}Ni mass $M_{\rm Ni}$ ($M_{\odot}$). *Middle panel*: $L_{\rm peak}$ vs. the parameter $M_{\rm ej}^3/E_{\rm k}$ derived from the ejecta mass $M_{\rm ej}$ and the kinetic energy $E_{\rm k}$. *Bottom panel*: $M_{\rm Ni}$ vs. $M_{\rm ej}^3/E_{\rm k}$. SN 2011kl is an extreme event in all three plots.

4.1.3. Powering SN 2011kl

An alternative way to power a luminous SN is the interaction with a dense stellar wind or ejected shells of large mass, i.e. the CSM-interaction model. Such shells can be emitted shortly (on astronomical timescales) before the final core collapse and cause spectra to change from Type I to Type II at late times (e.g. SN 2014C, Milisavljevic et al. 2015b; SN 2004dk, Mauerhan et al. 2018; SN 2017ens, Chen et al. 2018, and SN 2017dio,

Kuncarayakti et al. 2018), and possibly even serve as an additional energy source powering SLSNe (e.g. the cases of iPTF13ehe, iPTF15esb, and iPTF16bad; Yan et al. 2015, 2017; Liu et al. 2018a; Wang et al. 2016a). The possibility of such an interaction without the usual spectral signatures of H and He, which are clearly not detected (L14; G15; Krühler et al. 2015; Mazzali et al. 2016), has been discussed in the literature (e.g. Blinnikov & Sorokina 2010; Chevalier & Irwin 2011; Chatzopoulos & Wheeler 2012), and observed in at least one case (Ben-Ami et al. 2014), but these models have not been discussed in the context of GRB progenitors and have multiple issues when compared with our light-curve evolution. Furthermore, the detailed spectroscopic modelling strongly rules out any sign of interaction (G15; Mazzali et al. 2016). In G15, we arrived at the conclusion that SN 2011kl is a lower luminosity analogue to SLSNe powered by magnetar energy injection, implying that the central engine of GRB 111209A was itself a rapidly spinning magnetar. We note that one proposed indicator for a magnetar central engine, an early shock breakout (Kasen et al. 2016), would be hidden beneath the bright afterglow which is much more luminous than SN 2011kl even at peak. Further analysis of our data by other teams has yielded results which are in agreement with ours (Metzger et al. 2015; Bersten et al. 2016; Liu et al. 2017b; Cano et al. 2016; Wang et al. 2017a). Cano et al. (2016) even stated that the afterglow of GRB 111209A can be powered by magnetar emission. However, similar to Gompertz & Fruchter (2017), they only used the late afterglow data presented in G15. We note that recently it has been proposed, in contrast to the main conclusion of Cano et al. (2016), that many Type Ic-BL SNe may be mostly powered by magnetars (Wang et al. 2016b, 2017c,b); see Taddia et al. (2019b) for an observational example.

4.1.4. SN 2011kl, rapidly rising gap transients, and other luminous SNe

Arcavi et al. (2016) recently presented the discovery of several luminous transients, one of which has been spectroscopically confirmed as a SN. The other three are very likely SNe as well. They label these sources RRGTs, as they rise rapidly to peak luminosity (especially compared with SLSNe) and their peak luminosities are situated between those of usual SE-SNe (and even SNe Type Ia) and SLSNe, a parameter space where few events are known so far. Moriya et al. (2016) presented a model in which a supramassive neutron star (NS) collapses to a BH before expending much of its rotational energy, explaining the lower luminosity and more rapid late decline compared to SLSNe. Arcavi et al. (2016) drew a link to the similarly luminous and distant SN 2011kl (see Fig. 4), which would be the first reported RRGT if these events are indeed a distinct class. One source, SNLS06D1hc, stands out especially as its light-curve evolution is very similar to that of SN 2011kl (Fig. 2). Arcavi et al. (2016) provide an in-depth discussion on how the RRGTs compare to SN 2011kl (based partially on the bolometric values from G15), but we make a few points in this section. PTF10iam is the only source which is spectroscopically confirmed to be a SN. It is formally classified a Type II SN based on a high-velocity feature interpreted as Hα. The G15 authors found no evidence for H and He in the spectrum of SN 2011kl, and the H emission lines can be explained completely by host-galaxy emission linked to star formation (Krühler et al. 2015). Arcavi et al. (2016) found no GRBs linked to these events, although they only performed a catalogue search. GRB 111209A, while very energetic, had a low peak luminosity and did not trigger Konus-*WIND* (Golenetskii et al. 2011). Had *Swift* not triggered on the GRB, it is unclear when it would have been discovered; see the appendix of K18B for several untriggered extremely long GRBs, which were only detected much later by manual inspection. Therefore, such an archive inspection may yield detections of low-luminosity EL-GRBs, or at least stricter upper limits. GRB 111209A has one of the largest isotropic energy releases among $z < 0.9$ GRBs and may therefore be a bright outlier. The most similar event, SNLS06D1hc, has a single spectroscopic observation which yielded no significant SN features, but there may be a blue continuum superimposed upon the host-galaxy spectrum. The spectrum of SN 2011kl would have been very hard to disentangle from the spectrum of its host galaxy if the host had had a similar luminosity to that of SNLS06D1hc, therefore we may be seeing a SN 2011kl-like spectrum in this case as well. The hosts of the three RRGTs, except SNLS06D1hc, show roughly solar metallicities that are much higher than in the case of SN 2011kl. The metallicity of the host of SNLS06D1hc could not be measured, but the SFR is low, again in contrast to the host of GRB 111209A/SN 2011kl. All RRGT hosts also show evidence of evolved stellar populations.

In recent years, large surveys have begun to fill the gap. Aside from the fainter SLSNe mentioned above, a heterogenous population is being revealed. A few examples consist of the slowly evolving Type Ic SN 2012aa (Roy et al. 2016), the rapidly evolving, very blue Type Ibn ASASSN-14ms (Vallely et al. 2018), the extremely fast broad-lined Type Ic-BL iPTF16asu (Whitesides et al. 2017), and the spectroscopically evolving ASASSN-15no (Benetti et al. 2018).

These transients and those Arcavi et al. (2016) detected are clearly rare, and there are some intriguing similarities to SN 2011kl, just as there are clear differences, especially concerning the progenitor environments. Therefore, it already seems erroneous to lump all these transients into a separate class. Upcoming high-etendue optical surveys such as the Zwicky Transient Facility (Smith et al. 2014) and the Large Synoptic Survey Telescope (Tyson 2002) will find more of these transients.

4.2. Nature of GRB 111209A

The extreme duration of the prompt emission of GRB 111209A and the shape of the X-ray light curve and the early optical data led to the speculation that this event might be similar to low-luminosity XRF 060218/SN 2006aj, to the Christmas Burst GRB 101225A, or the relativistic tidal disruption flares (RTDFs) GRB 110328A/Swift J164449.3+573451 and Swift J2058.4+0516 (Gendre et al. 2013; L14). From our data and analyses, as given in G15, K18B, and in this work, we find multiple large differences to these events which point to GRB 111209A not being related to these types of gamma-ray transients.

The energetics and spectral parameters of the prompt emission are, other than the extreme duration, typical for long GRBs (Golenetskii et al. 2011). Even the light-curve shape, while strongly stretched, is similar to a typical bright, multi-peaked GRB. This is in stark contrast to the very soft and temporally simple prompt emission of XRF 060218 or XRF 100316D. We note, however that the extreme duration implies a variability timescale that is more comparable to the aforementioned XRFs than to typical high-luminosity GRBs. GRB 111209A is followed by an afterglow which is, while showing some complicated temporal and spectral evolution, in general very similar to typical GRB afterglows. We derived that the optical luminosity lies close to the mean of the known afterglow luminosity distribution (K18B), and the SED shows a nearly

straight and red spectral slope with low extinction (K18B). This again agrees fully with normal afterglows, and is very different from the evolving thermal spectrum seen in the afterglow of GRB 101225A (Thöne et al. 2011) or the very blue and hot thermal spectrum seen for RTDF Swift J2058.4+0516 (Cenko et al. 2012) and implied for GRB 110328A/Swift J164449.3+573451, which was obscured behind significant rest-frame extinction (Levan et al. 2011). The event is also in agreement with typical GRBs in the optical luminosity vs. isotropic energy release plane (Kann et al. 2010). We detect a slow (in comparison with typical GRB-SNe), very luminous, and exceptionally blue SN following the GRB, which agrees very well with the prototypical GRB-SN 1998bw in terms of temporal evolution, although it looks different from typical GRB-SNe spectrally (G15). GRB 101225A was probably also followed by a SN, which must be more luminous than the value given in Thöne et al. (2011), in consideration of the higher spectroscopic redshift (L14), and no SN is expected in the case of RTDFs. The L14 authors already came to the conclusion that it is unlikely that GRB 111209A originated in a RTDF. But since their data are ambiguous in terms of the detection of a SN signature, they were not able to rule out the RTDF origin; whereas we feel we are now able to do so in the light of our luminous SN signature and the standard GRB afterglow (K18B, see also G15). The offset from the core of the host galaxy is very small (especially as measured by L14), which is in agreement with a RTDF model; but, as L14 stated, is also not in disagreement with a GRB origin (e.g. from a nuclear starburst in a very compact dwarf host galaxy).

Evans et al. (2014) presented a detailed discussion of the prompt emission and afterglow (in X-rays) of GRB 130925A, which we also studied concerning its (optical)/NIR emission (K18B). They also found strong evidence that GRB 130925A is not due to a tidal disruption event (TDE)/RTDF. In the GRB context, they explained the long prompt emission (see the appendix of K18B for more details) as being due to a very low circumburst medium density, this implies a very large deceleration radius R_d of the jet. Shells with differing Lorentz factors therefore have more time to collide, producing internal shocks and therefore prompt gamma-ray emission, before reaching R_d and the forward shock. Shells that arrive at even later times are not able to interact any more and just contribute to the external forward shock in the form of energy injections, of which we actually detected several in the late-time afterglow of GRB 111209A (K18B). We also found possible evidence of a very low circumburst medium density in the case of GRB 111209A (K18B; but see the arguments in Gompertz & Fruchter 2017).

While this explanation therefore also seems attractive in the case of GRB 111209A, we point out several differences to GRB 130925A. For one, the forward shock was extremely faint for the latter burst, the "afterglow" can be explained entirely by a dust echo (Evans et al. 2014). While Evans et al. (2014) state that the case is similar for GRB 111209A and another ULGRB, GRB 121027A (see appendix of K18B), they do not find significant spectral evolution in the X-ray afterglows of the two latter GRBs, pointing to a standard external-shock origin of their afterglows. Furthermore, we found (K18B) that the optical afterglow of GRB 111209A, while not being highly luminous, is comparable to those of many other GRBs – and even to some with extremely luminous prompt emission; see Fig. 8 of Kann et al. (2010) for examples of GRBs with large $E_{\rm iso}$ and, relatively speaking, faint afterglows. This is also true for the X-ray afterglow (Gendre et al. 2013). The detection of bright radio emission several days after the GRB (Hancock et al. 2012) also indicates that the circumburst medium density cannot be exceptionally low.

A second difference stems from the prompt emission pulses. GRB 130925A, as shown by Evans et al. (2014), exhibits a very large number (~40) of pulses; in general, the GRB resembles typical prompt emission, but it is ongoing for a very long time. GRB 111209A, on the other hand, shows a very slowly varying envelope. Such extremely slow variation would point to a large emission region (and thus a low circumburst-medium density, so that shells collide at large radii), as shown by Barnacka & Loeb (2014) that is even more extreme than in the case of GRB 130925A. This very large so-called minimum timescale (MTS) would also point to a very low Lorentz factor (Sonbas et al. 2015), but this is incompatible with opacity arguments; we note that the peak energy of the prompt emission is >500 keV. On the other hand, the MTS of GRB 111209A likely lies significantly above all the values plotted in Sonbas et al. (2015), so it is unclear how the relationship of these authors would apply.

Margutti et al. (2015) posited a direct physical connection between extremely long prompt emission duration and high circumburst X-ray column densities as well as very soft late X-ray afterglows which indicate reprocessing of X-ray emission from the forward shock. They only studied GRBs at $z < 0.5$ and found the following four examples: XRFs 060218 and 100316D, and the two GRBs 090417B and 130925A, which are both bona fide dark GRBs. Owing to the redshift cut-off, GRB 111209A was not included. This burst shares some of the aspects of their sample (obviously, the ultra-long duration and the very long variability timescale), but is markedly different in others. Using the tools of the XRT on-line repository (Evans et al. 2007, 2009), we find that the X-ray afterglow, using only data after 100 ks, has a somewhat softer spectrum ($\Gamma = 2.50^{+0.20}_{-0.18}$) than expected for a forward-shock-driven afterglow, but is not in the same region as the Margutti sample (all $\Gamma > 3$); also, as mentioned above, there is no spectral evolution detected. The equivalent hydrogen column density as measured from X-rays, $N_{\rm H} = 2.5^{+1.1}_{-1.0} \times 10^{21}$ cm^{-2}, is typical for GRB afterglows, and as we show in K18B, the line-of-sight extinction in the optical is low. GRB 111209A lies in the top right hand quadrant of Fig. 2 of Margutti et al. (2015) as do the other very long GRBs they have studied, but it lies significantly below the rest of the sample. Furthermore, the prompt emission of GRB 111209A shows a much higher peak energy than any of the cases in the sample of Margutti et al. (2015). Therefore, if there is indeed a physical link between an extremely long prompt-emission duration and the pre-explosion mass-loss history of the progenitor, it seems less likely that this link also applies to the case of GRB 111209A; the extreme duration is more likely to be intrinsic than a result of a complex mass-loss environment (Margutti et al. 2015).

Thanks to the classification of the spectrum of SN 2011kl as being driven by the energy release from a magnetar (G15), it would seem we can narrow down the possibilities, and the extreme duration of the prompt emission could be directly linked to the existence of a magnetar central engine. The exact connection remains unclear, however. Magnetars as central engines of GRBs have been invoked multiple times. XRF 060218 has been invoked as an example of a magnetar-powered GRB (Mazzali et al. 2006), but its prompt emission, while very long, differs strongly from that of GRB 111209A, and the associated SN 2006aj shows no signs of being anything but a Type Ic-BL SN powered by radioactive decay (e.g. Pian et al. 2006). Magnetars have also been used to explain a rarely seen phenomenon of a long-lasting X-ray plateau followed by a very steep decay at late times (Zhang & Mészáros 2001). In this scenario, the

optical afterglow behaves completely differently, of which prime examples are GRBs 070110 (Troja et al. 2007) and 130831A (De Pasquale et al. 2016b). These GRBs were otherwise completely unremarkable; GRB 130831A was also followed by a garden-variety Type Ic-BL SN, SN 2013fu (Cano et al. 2014; Klose et al. 2019). Therefore, even though this paper, together with G15 and K18B, shows strong evidence for a GRB central engine not involving a rapidly spinning BH, the exact connection between the ultra-long duration and the spectrally deviant, luminous SN remains a topic for further research.

4.3. Literature on GRB 111209A in light of our complete data set

GRB 111209A and long-lasting gamma-ray transients in general have been much-discussed in the literature in recent years. Most of the studies pertaining to GRB 111209A were based on significantly incomplete data sets.

4.3.1. Models for gamma-ray transients of extreme duration

Quataert & Kasen (2012) and Woosley & Heger (2012) studied the possibility of explaining long-duration γ-ray transients, such as those GRB 111209A has been postulated to resemble (Sect. 4.2), through the long-term accretion of the outer layers of massive stars, generally those that have not experienced envelope-stripping. Such transients are unable to explain GRB 111209A. Most models lead to low-luminosity emission which lasts dozens, if not hundreds of days. Hereby, the emitted luminosity would lie one to two orders of magnitude below that of GRB 111209A. While a BSG progenitor would lead to an emission time in agreement with GRB 111209A (10^4–10^5 s, Woosley & Heger 2012), it is expected to be even less luminous than a red supergiant progenitor. Furthermore, in contrast to the bright SN we discovered, these Type 3 collapsars, as labelled by Woosley & Heger (2012), would also very likely not be accompanied by SN emission; as such a SN would detach precisely the outer layers needed for accretion.

Quataert & Kasen (2012) also contemplated if a millisecond magnetar central engine, which in general has been posited to be a valid central engine model for GRBs (e.g. Metzger et al. 2011, and references therein), is able to power a long-duration low-luminosity γ-ray transient, and found that the magnetic field strength must lie under that of typical magnetars to enable a much slower spin-down and therefore a longer emission period. Again, such a transient would be much longer and fainter than GRB 111209A, but there is no argument against scaling up the magnetic field to a value between the classic millisecond magnetar central engine which emits most of its energy on the timescale of typical long GRBs, and the scenario which Quataert & Kasen (2012) proposed. Such a scenario is discussed in the light of the spectrum of SN 2011kl presented in G15, although caveats in terms of variability and energetics remain (Sect. 4.2; see also e.g. Gompertz & Fruchter 2017).

Janiuk et al. (2013a,b) proposed a scenario in which the exploding progenitor is in a tight orbit with a second stellar-mass BH. Shortly after exploding as a SN, the two BHs merge, and additional accretion powers a second episode of ultrarelativistic jet launching, leading to a very long-duration GRB. While such a model may explain so-called "double bursts" such as GRB 110709B (Zhang et al. 2012) and GRB 121217A (Siegel et al. 2013; Elliott et al. 2014), it is unlikely to explain the sustained and extremely extended, but low-peak-flux emission of GRB 111209A.

Nathanail & Contopoulos (2015) presented a model in which ULGRBs are explained by delayed accretion on to a BH engine; the delay is achieved by a magnetic field strength that is lower than usual. Such a model would be in contrast to the magnetar scenario (G15), but Nathanail & Contopoulos (2015) conceded that is possible for a magnetar to work within their model.

Gilkis et al. (2016) studied core-collapse SNe in general within the framework of the jittering-jets model, and proposed that for progenitors with very high pre-collapse angular momentum (generally seen as a prerequisite for GRBs), strong collimated polar outflows are created, as well as a slow equatorial outflow which partially forms a massive and extended accretion disc. Such a disc, they proposed, could continue the jet-emission process, thereby powering the SN to SLSN luminosities. Furthermore, if the accretion time is measured in hours to days, this would yield a natural explanation for ULGRBs and possibly also for the high luminosity of an associated SN, and for RRGTs that Arcavi et al. (2016) studied. It remains to be seen whether such a model would yield the specific spectral shape of SN 2011kl (G15). We furthermore note that the model of Gilkis et al. (2016) predicted definite asymmetries in the explosion, but polarimetry studies of SLSNe so far have yielded null results (Leloudas et al. 2015b; Brown et al. 2016; Cikota et al. 2018; Maund et al. 2019) with some exceptions (Inserra et al. 2016; Leloudas et al. 2017; Bose et al. 2018).

Perets et al. (2016) discussed what they call micro TDEs (μTDEs), in which planetary-mass objects or solar-mass stars are tidally disrupted by stellar-mass BHs. These authors found that in the case of solar-type stars, where the mass ratio is $\approx$0.1 (or even higher), jet production may set in, and a long-lasting gamma-ray flare is produced, whose duration and energetics agree well with ULGRBs. While μTDEs in general would not produce any SN emission, they also envisioned a special scenario in which a massive star explodes as a SN, producing the compact object, whose natal kick brings it close to a wide companion, thereby producing the μTDE just hours or days after the SN detonation. They mentioned GRB 111209A/SN 2011kl as a possible candidate for such a scenario. Still, there is no obvious way to explain why SN 2011kl has the measured properties, in terms of luminosity and spectral shape. Furthermore, it is unclear if such a scenario can produce a classical GRB jet which then causes a standard afterglow as in the case of SN 2011kl. The agreement of SN 2011kl with the SN 1998bw template indicates that GRB 111209A and the SN are likely contemporaneous, but a delay of a few hours does not disagree with the data. Surprisingly, in this case the SN would precede the GRB. Perets et al. (2016) found that BHs make better compact objects for the creation of μTDEs, but a NS, and possibly even a magnetar, is not ruled out. We may even envision that the secondary accretion event could spin up the NS further, increasing the energy reservoir needed to power the SN to its high luminosity. Therefore, while the scenario seems very fine-tuned, it remains an interesting candidate which should be further explored.

Gao et al. (2016) presented an alternate model in which GRB 111209A is powered by fall-back accretion on to a BH central engine, which would explain the ultra-long duration. Furthermore, the fall-back accretion disc should then power the high luminosity (and possibly different spectral shape compared to the usual Type-Ic BL associated with GRBs) of SN 2011kl via the Blandford-Payne mechanism (Blandford & Payne 1982). It remains unclear whether such a mechanism can indeed reproduce the spectral peculiarities of SN 2011kl and whether a BH

fall-back process can extend long enough, after powering the ultra-long GRB, to also yield the power to produce the high SN luminosity (Metzger et al. 2015).

Beniamini et al. (2017) have studied the ability of magnetars, assuming different emission models, in powering GRBs. They found that T_{90} should typically be $\approx$100 s, in strong contrast to the existence of ULGRBs. They point out, however, that the prompt emission time may be enhanced if the jet entrains a significant baryon loading when passing through the star. Additionally, further fall-back accretion may increase the energy output of the magnetar and produce a longer emission timescale as well.

The case of fall-back accretion on to a proto-magnetar is further studied by Metzger et al. (2018), who indeed find that under certain circumstances, such fall-back can hold the magnetization at a critical level to enable prompt emission times in the range of thousands of seconds, while at the same time still being able to power the accompanying SN to luminosities exceeding those achievable by ^{56}Ni decay alone; such a proto-magnetar would also produce typical amounts of ^{56}Ni right after core-collapse. This model therefore represents one of the best solutions for GRB 111209A/SN 2011kl presented so far.

Liu et al. (2018b) used prompt emission data to constrain the possible progenitor stars of GRBs of different duration within the framework of a BH hyper-accretion model. They found that ULGRBs such as GRB 111209A can only have progenitors of high mass and low metallicity, up to metal-free Pop III stars. While this model is similar to the standard model and therefore an accompanying SN is expected, it does not explain the specific properties of SN 2011kl, which point to a magnetar origin.

Perna et al. (2018) have used multi-code numerical modelling to evolve a low-metallicity, massive star to a BSG end phase, and then produce a long-lasting, ultra-relativistic jet which is able to drill through the extended envelope and produce an ULGRB of $\approx$10 ks duration if seen near axis. While this modelling shows that BSG progenitors are able to produce ULGRBs, it does not encompass the creation of the SN or explain its high luminosity and spectral properties. We also note this model uses a BH central engine.

Aguilera-Dena et al. (2018) have presented evolutionary models of potential Type Ic progenitor stars that reach large C/O-core masses via enhanced mixing. Depending on the core mass, they found a continuum spanning from Type Ic SLSNe over magnetar-powered GRB-SNe, BH powered GRB-SNe up to PPI-SNe. The potential magnetar-powered GRB-SNe are found near the NS/BH boundary, implying very massive, rapidly rotating NSs (see K18B for more discussion about the cumulative energetics of the event). Aguilera-Dena et al. (2018) have mentioned this part of the parameter space as a potential progenitor for GRB 111209A.

4.3.2. GRB111209A: Then and now

Gendre et al. (2013) presented a detailed study of the GRB 111209A prompt emission, mostly in γ-rays and X-rays. They ruled out an origin of GRB 111209A in a SN shock breakout (lack of a strong thermal component, energetics), a magnetar origin (discrepancy between energy release and prompt-emission peak energy, light-curve behaviour in X-rays), and a RTDF origin (light-curve behaviour in X-rays). Concerning the latter, we note that Gendre et al. (2013) also cited the lack of a host galaxy as a counterargument against a RTDF origin, whereas both L14 and K18B presented host-galaxy detections, and L14 argued that the host is still massive enough to contain a central supermassive BH that can create a RTDF. Finally, Gendre et al. (2013) came to the conclusion that the only model supported by their data is that of the core collapse of a single low-metallicity supergiant star, a BSG. They based this decision on the apparent lack of any SN detection for GRB 111209A, as, at the time of writing of their manuscript, only a preliminary analysis of the data set presented in L14 had been made public. The final analysis of L14 revealed indications of an accompanying SN, and our own observations (G15; K18B) show that not only does the SN signature exist, it is highly luminous, in contrast to the expectations of the model of Woosley & Heger (2012) and therefore Gendre et al. (2013), as already stated above. Additional arguments against a low-metallicity BSG progenitor were made by L14 (host-galaxy metallicity; but see Krühler et al. 2015) and Stratta et al. (2013, detection of dust along the GRB line of sight), the latter argument is also confirmed in K18B. Gao et al. (2016), while favouring a BH-powered model, also ruled out an extended star as a progenitor.

Kashiyama et al. (2013) developed models for an optical transient phenomenon they labelled Cocoon Fireball Photospheric Emission (CFPE), which can create luminous, long-lasting transients peaking in the optical regime from massive BSG progenitors (e.g. luminous blue variables or even Population III stars). Because of the link to a possible BSG progenitor for GRB 111209A that Gendre et al. (2013) had posited, Kashiyama et al. (2013) also modelled what such a transient would look like at the redshift of GRB 111209A (their Fig. 6). This transient would peak around the 26th–25th magnitude, depending on the zero-age main sequence mass of the progenitor; would have a peak time of $\approx 2\text{–}2.5 \times 10^7$ s (several hundred days); and would have a very blue spectrum rising towards the ultraviolet, therefore the opposite of an afterglow or typical SN spectrum. Together with the late observations of L14, we have only two epochs spanning this late time. No significant variability is detected in $g'r'$ between 200 and 280 days. We note that the transient Kashiyama et al. (2013) found in their models has a roughly symmetrical magnitude evolution in log space and may therefore peak in between the two epochs; the lack of variability would be a chance effect of the temporal spacing. Therefore, we are unable to exclude significantly the existence of such a transient. The additional component we find at $\approx$ tens of days after the GRB is much faster and much more luminous than the CFPEs Kashiyama et al. (2013) found in their model, and therefore very unlikely to be due to this phenomenon. Furthermore, as we argued previously, it is unlikely that the progenitor is a BSG, and therefore the model of Kashiyama et al. (2013) would not be applicable anyway. They also derived models for CFPEs of exploding Wolf–Rayet stars, but these are several magnitudes fainter than the BSG CFPEs and would be completely undetectable in our data, being far less luminous than even the faint host galaxy of GRB 111209A.

Nakauchi et al. (2013) expanded upon the work of Kashiyama et al. (2013), fitting new CFPE models to the data presented by L14. They found that using a certain set of initial parameters, they are able to reproduce the red rebrightening seen especially in the J band data of L14, which they claim to be about an order of magnitude more luminous than typical GRB-SNe, and therefore SLSN-like. While we find the observer-frame J-band SN to be several times more luminous than SN 1998bw in the same band, this is still below the regime of SLSNe. Comparing our data with the model light curves of Nakauchi et al. (2013) shows that their model significantly exceeds our data in luminosity, and additionally there is no evidence for the very

steep decay they found. Therefore, if the rebrightening following GRB 111209A is to be explained by such a modified CFPE, the initial parameters must be very different from those chosen by Nakauchi et al. (2013). We note that these authors agreed with Kashiyama et al. (2013) in that CFPEs of Wolf–Rayet stars would be too faint to detect, such an effect is clearly ruled out by our data.

Ioka et al. (2016) applied three different models to the GROND data of GRB 111209A/SN 2011kl: a BSG model, a magnetar model, and a model involving a TDF caused by a relatively low-mass supermassive BH destroying a white dwarf (WD). These authors claimed that all three models can fit the data, but favoured especially the WD-TDF model and found problems with the parameters of the magnetar model. In their paper, they only employed the GROND data as presented in G15, thereby ignoring the rebrightening episode, the complex early afterglow, and the multiple smaller rebrightenings in the late afterglow. Furthermore, they did not show residuals of their fits or give χ^2 values. Visual inspection of their fits reveals strong offsets between data and fit curves in some colours, and it is unclear whether their models can match the spectrally determined colours of SN 2011kl. We therefore conclude that as it stands, their modelling does not present a strong argument against the magnetar model for SN 2011kl. We also note that other authors, for instance Yu et al. (2017), have derived magnetar-model parameters which are unexceptional and in agreement with those of, for example SLSNe (see Sect. 4.1.3). Wang et al. (2017a) have also used the bolometric light-curve decomposition of Ioka et al. (2016) and have found it can be fit with a ^{56}Ni+magnetar+cooling envelope model, without the need for a BSG or WD-TDF model.

5. Conclusions

In a series of papers, we have studied the ULGRB 111209A. In G15, we presented the discovery of the highly luminous SN 2011kl accompanying GRB 111209A, a remarkable event that is spectrally more similar to SLSNe. In K18B, we studied the entire optical/NIR afterglow of GRB 111209A and find a complex evolution. But, in contrast to SN 2011kl, we find no features that set it apart from the known sample of GRB afterglows.

In this work, we study SN 2011kl within the context of large SE-SN, GRB-SN, and SLSN samples. We derive a bolometric light curve including NIR corrections, confirming and expanding upon the results of G15 that if this SN would be powered by ^{56}Ni it would be a significant outlier compared to all known (non-SLSN) SE-SNe. At the same time, in terms of luminosity and rapidity of light-curve evolution, SN 2011kl is also an outlier compared to the SLSN sample which it resembles spectroscopically (G15; Mazzali et al. 2016) because it is less luminous and faster and inhabits the luminosity gap between GRB-SNe and SLSNe; only a few more sources have been found in this luminosity gap so far (e.g. Arcavi et al. 2016), some of which are spectrally confirmed SLSNe (De Cia et al. 2018; Lunnan et al. 2018a; Quimby et al. 2018). All in all, SN 2011kl is a true hybrid and represents a transition object between the rapidly expanding SE-SNe accompanying GRBs and the highly luminous SLSNe.

Even in the light of our studies, a complete explanation for GRB 111209A/SN 2011kl is still lacking. Is a magnetar capable of powering the entire event (Gompertz & Fruchter 2017; K18B)? Is this truly necessary or are certain elements, such as the afterglow, powered by conventional mechanisms known from standard GRBs (e.g. deceleration by the circumburst medium and synchrotron radiation from a forward shock in the case of the afterglow)? Is the ultra-long prompt emission phase related to accretion of similar duration or is it produced by interaction with the environment (Evans et al. 2014)?

So far, very few ULGRBs are known, and this is the first exhibiting an accompanying SN, which at first glance links it to normal long GRBs. A more detailed analysis has revealed several striking differences, indicating that we as yet have not discovered the entire "bestiary" of gamma-ray transients in the Universe. Any further similar events in the future need to be followed up with all possible effort, but their low gamma-ray peak fluxes and long-scale variability may bias these events against detection, especially at higher redshifts.

Lately, evidence has been growing that there is a continuum of SE-SNe reaching from Types IIb, Ib, Ic over Type Ic-BL, and GRB-SNe (e.g. Mazzali et al. 2008), possibly due to common jet physics (e.g. Piran et al. 2019; Sobacchi et al. 2017b; Petropoulou et al. 2017; Soker & Gilkis 2017). Evidence suggests this continuum continues all the way to SLSNe-I, possibly because of envelope properties (Sobacchi et al. 2017a), magnetar-axes alignment (Margalit et al. 2018a,b), magnetar field strength (Yu et al. 2017), or C/O core mass at explosion time (Aguilera-Dena et al. 2018). Similarities have been found in the spectral properties both in the photospheric (Liu et al. 2017b; Blanchard et al. 2019) and nebular (e.g. Milisavljevic et al. 2013; Nicholl et al. 2016a; Jerkstrand et al. 2017) phases. Spectroscopically classified SLSNe have been discovered to populate the luminosity gap (De Cia et al. 2018; Lunnan et al. 2018a; Quimby et al. 2018; Angus et al. 2018), X-ray observations reveal similar environments (Margutti et al. 2018), and there are indications from simulations (Suzuki & Maeda 2017) as well. All in all, there are more and more indications for the existence of a connection between GRBs and SLSNe (Margalit et al. 2018b). While a connection between SLSNe and highly stripped progenitors was quickly established (Pastorello et al. 2010), a connection to GRBs was hardly obvious and has been forthcoming more slowly. GRB 111209A/SN 2011kl may ultimately turn out to be the first missing link between classical GRBs and SLSNe to be discovered; in a case where it was not, at the time, suspected that such a missing link was even needed. The final step would now be to discover a high signal-to-noise, spectroscopically indubitable SLSN even if it does not make the luminosity cut, which is clearly associated with a GRB, be it of ultra-long duration or not.

Acknowledgements. DAK wishes to dedicate these works to his father, R.I.P. 20. 08. 2015. You are sorely missed by so many. DAK acknowledges Zach Cano, Massimiliano De Pasquale, Daniele Malesani, Antonio de Ugarte Postigo, Christina C. Thöne, Bing Zhang, Thomas Kampf, Cristiano Guidorzi, Raffaella Margutti, and Ting-Wan Chen for interesting discussions and helpful comments. DAK also thanks A. Sagues Carracedo for further information on the bolometric light curve of SN 2017iuk. DAK acknowledges financial support by the DFG Cluster of Excellence "Origin and Structure of the Universe," from MPE, from TLS, from the Spanish research project AYA 2014-58381-P, and from Juan de la Cierva Incorporación fellowship IJCI-2015-26153. We are indebted to Joe Lyman and Vicki Toy for supplying the bolometric light curves of GRB 120422A/SN 2012bz and GRB 130702A/SN 2013dx, respectively. SK, DAK, ARossi, and ANG acknowledge support by DFG grants Kl 766/16-1 and Kl 766/16-3, SSchmidl also acknowledges the latter. ARossi acknowledges support from the Jenaer Graduiertenakademie and by the project PRIN-INAF 2012 "The role of dust in galaxy evolution". TK acknowledges support by the DFG Cluster of Excellence Origin and Structure of the Universe, and by the European Commission under the Marie Curie Intra-European Fellowship Programme. RF acknowledges support from European Regional Development Fund-Project "Engineering applications of microworld physics" (No. CZ.02.1.01/0.0/0.0/16_019/0000766). DARK is funded by the DNRF. FOE acknowledges funding of his Ph.D. through the DAAD, and support from FONDECYT through postdoctoral grant 3140326. SSchulze acknowledges support from CONICYT-Chile FONDECYT 3140534, Basal-CATA PFB-06/2007,

and Project IC120009 “Millennium Institute of Astrophysics (MAS)” of Iniciativa Científica Milenio del Ministerio de Economía, Fomento y Turismo. SK, SSchmidl, and ANG acknowledge support by the Thüringer Ministerium für Bildung, Wissenschaft und Kultur under FKZ 12010-514. MN and PS acknowledge support by DFG grant SA 2001/2-1. ANG, DAK, ARossi and AU are grateful for travel funding support through MPE. Part of the funding for GROND (both hardware as well as personnel) was generously granted from the Leibniz-Prize to Prof. G. Hasinger (DFG grant HA 1850/28-1). This work made use of data supplied by the UK Swift Science Data Centre at the University of Leicester.

References

Aguilera-Dena, D. R., Langer, N., Moriya, T. J., & Schootemeijer, A. 2018, ApJ, 858, 115
Anderson, J. P., Pessi, P. J., Dessart, L., et al. 2018, A&A, 620, A67
Angus, C. R., Smith, M., Sullivan, M., et al. 2018, MNRAS, submitted [arXiv:1812.04071]
Arcavi, I., Wolf, W. M., Howell, D. A., et al. 2016, ApJ, 819, 35
Arnett, W. D. 1982, ApJ, 253, 785
Ashall, C., Pian, E., Mazzali, P. A., et al. 2017, Nat. Astron., submitted [arXiv:1702.04339]
Barkat, Z., Rakavy, G., & Sack, N. 1967, Phys. Rev. Lett., 18, 379
Barnacka, A., & Loeb, A. 2014, ApJ, 794, L8
Barnes, J., Duffell, P. C., Liu, Y., et al. 2018, ApJ, 860, 38
Ben-Ami, S., Gal-Yam, A., Mazzali, P. A., et al. 2014, ApJ, 785, 37
Benetti, S., Nicholl, M., Cappellaro, E., et al. 2014, MNRAS, 441, 289
Benetti, S., Zampieri, L., Pastorello, A., et al. 2018, MNRAS, 476, 261
Beniamini, P., Giannios, D., & Metzger, B. D. 2017, MNRAS, 472, 3058
Bersten, M. C., Benvenuto, O. G., Orellana, M., & Nomoto, K. 2016, ApJ, 817, L8
Bhirombhakdi, K., Chornock, R., Margutti, R., et al. 2018, ApJ, 868, L32
Blanchard, P. K., Nicholl, M., Berger, E., et al. 2018, ApJ, 865, 9
Blanchard, P. K., Nicholl, M., Berger, E., et al. 2019, ApJ, 872, 90
Blandford, R. D., & Payne, D. G. 1982, MNRAS, 199, 883
Blinnikov, S. I., & Sorokina, E. I. 2010, ArXiv e-prints [arXiv:1009.4353v2]
Bloom, J. S., Kulkarni, S. R., Djorgovski, S. G., et al. 1999, Nature, 401, 453
Bloom, J. S., Perley, D. A., Li, W., et al. 2009, ApJ, 691, 723
Bose, S., Dong, S., Pastorello, A., et al. 2018, ApJ, 853, 57
Brown, G. C., Levan, A. J., Stanway, E. R., et al. 2015, MNRAS, 452, 4297
Brown, P. J., Yang, Y., Cooke, J., et al. 2016, ApJ, 828, 3
Bufano, F., Pian, E., Sollerman, J., et al. 2012, ApJ, 753, 67
Cano, Z. 2013, MNRAS, 434, 1098
Cano, Z., Bersier, D., Guidorzi, C., et al. 2011, MNRAS, 413, 669
Cano, Z., de Ugarte Postigo, A., Pozanenko, A., et al. 2014, A&A, 568, A19
Cano, Z., Johansson Andreas, K. G., & Maeda, K. 2016, MNRAS, 457, 2761
Cano, Z., Wang, S.-Q., Dai, Z.-G., & Wu, X.-F. 2017a, Adv. Astron., 2017, 8929054
Cano, Z., Izzo, L., de Ugarte Postigo, A., et al. 2017b, A&A, 605, A107
Cenko, S. B., Krimm, H. A., Horesh, A., et al. 2012, ApJ, 753, 77
Chatzopoulos, E., & Wheeler, J. C. 2012, ApJ, 760, 154
Chatzopoulos, E., Wheeler, J. C., Vinko, J., Horvath, Z. L., & Nagy, A. 2013, ApJ, 773, 76
Chen, T.-W., Smartt, S. J., Bresolin, F., et al. 2013, ApJ, 763, L28
Chen, T.-W., Smartt, S. J., Jerkstrand, A., et al. 2015, MNRAS, 452, 1567
Chen, T.-W., Schady, P., Xiao, L., et al. 2017a, ApJ, 849, L4
Chen, T.-W., Nicholl, M., Smartt, S. J., et al. 2017b, A&A, 602, A9
Chen, K.-J., Moriya, T. J., Woosley, S. E., et al. 2017c, ApJ, 839, 85
Chen, T.-W., Inserra, C., Fraser, M., et al. 2018, ApJ, 867, L31
Chevalier, R. A., & Irwin, C. M. 2011, ApJ, 729, L6
Chomiuk, L., Chornock, R., Soderberg, A. M., et al. 2011, ApJ, 743, 114
Cikota, A., Leloudas, G., Bulla, M., et al. 2018, MNRAS, 479, 4984
Clocchiatti, A., Suntzeff, N. B., Covarrubias, R., & Candia, P. 2011, AJ, 141, 163
Cobb, B. E., Bloom, J. S., Perley, D. A., et al. 2010, ApJ, 718, L150
Cooke, J., Sullivan, M., Gal-Yam, A., et al. 2012, Nature, 491, 228
Coppejans, D. L., Margutti, R., Guidorzi, C., et al. 2018, ApJ, 856, 56
Corsi, A., Cenko, S. B., Kasliwal, M. M., et al. 2017, ApJ, 847, 54
Curtin, C., Cooke, J., Moriya, T. J., et al. 2019, ApJS, 241, 17
D’Ai, A., Burrows, D. N., Cholden-Brown, A., et al. 2017, GRB CoordinatesNetwork, Circular Service, 21340, 21340
De Cia, A., Gal-Yam, A., Rubin, A., et al. 2018, ApJ, 860, 100
De Pasquale, M., Page, M. J., Kann, D. A., et al. 2016a, MNRAS, 462, 1111
De Pasquale, M., Oates, S. R., Racusin, J. L., et al. 2016b, MNRAS, 455, 1027
de Ugarte Postigo, A., Selsing, J., Malesani, D., et al. 2017, GRB CoordinatesNetwork, Circular Service, 22096, 22096
D’Elia, V., Pian, E., Melandri, A., et al. 2015, A&A, 577, A116
Della Valle, M., Malesani, D., Benetti, S., et al. 2003, A&A, 406, L33
Della Valle, M., Malesani, D., Bloom, J. S., et al. 2006, ApJ, 642, L103
Dong, S., Shappee, B. J., Prieto, J. L., et al. 2016, Science, 351, 257
Elliott, J., Yu, H.-F., Schmidl, S., et al. 2014, A&A, 562, A100
Evans, P. A., Beardmore, A. P., Page, K. L., et al. 2007, A&A, 469, 379
Evans, P. A., Beardmore, A. P., Page, K. L., et al. 2009, MNRAS, 397, 1177
Evans, P. A., Willingale, R., Osborne, J. P., et al. 2014, MNRAS, 444, 250
Ferrero, P., Kann, D. A., Zeh, A., et al. 2006, A&A, 457, 857
Filgas, R., Greiner, J., Schady, P., et al. 2011, A&A, 535, A57
Foley, S., Watson, D., Gorosabel, J., et al. 2006, A&A, 447, 891
Fraley, G. S. 1968, Ap&SS, 2, 96
Fryer, C. L., & Heger, A. 2005, ApJ, 623, 302
Fynbo, J. P. U., Sollerman, J., Hjorth, J., et al. 2004, ApJ, 609, 962
Gal-Yam, A. 2012, Science, 337, 927
Gal-Yam, A. 2018, ARA&A, submitted [arXiv:1812.01428]
Gal-Yam, A., Mazzali, P., Ofek, E. O., et al. 2009, Nature, 462, 624
Galama, T. J., Vreeswijk, P. M., van Paradijs, J., et al. 1998, Nature, 395, 670
Galama, T. J., Tanvir, N., Vreeswijk, P. M., et al. 2000, ApJ, 536, 185
Gao, H., Lei, W.-H., You, Z.-Q., & Xie, W. 2016, ApJ, 826, 141
Garnavich, P. M., Stanek, K. Z., Wyrzykowski, L., et al. 2003, ApJ, 582, 924
Gehrels, N., Chincarini, G., Giommi, P., et al. 2004, ApJ, 611, 1005
Gehrels, N., Norris, J. P., Barthelmy, S. D., et al. 2006, Nature, 444, 1044
Gehrels, N., Ramirez-Ruiz, E., & Fox, D. B. 2009, ARA&A, 47, 567
Gendre, B., Stratta, G., Atteia, J. L., et al. 2013, ApJ, 766, 30
Gilkis, A., Soker, N., & Papish, O. 2016, ApJ, 826, 178
Godoy-Rivera, D., Stanek, K. Z., Kochanek, C. S., et al. 2017, MNRAS, 466, 1428
Golenetskii, S., Aptekar, R., Mazets, E., et al. 2011, GCN Circulars, 12663
Gompertz, B., & Fruchter, A. 2017, ApJ, 839, 49
Greiner, J., Klose, S., Salvato, M., et al. 2003, ApJ, 599, 1223
Greiner, J., Bornemann, W., Clemens, C., et al. 2008, PASP, 120, 405
Greiner, J., Mazzali, P. A., Kann, D. A., et al. 2015, Nature, 523, 189
Hancock, P. J., Murphy, T., Gaensler, B., & Zauderer, A. 2012, GCN Circulars, 12804
Hjorth, J., Sollerman, J., Møller, P., et al. 2003, Nature, 423, 847
Howell, D. A., Kasen, D., Lidman, C., et al. 2013, ApJ, 779, 98
Huang, Y. F., Wu, X. F., Dai, Z. G., Ma, H. T., & Lu, T. 2004, ApJ, 605, 300
Inserra, C., Smartt, S. J., Jerkstrand, A., et al. 2013, ApJ, 770, 128
Inserra, C., Bulla, M., Sim, S. A., & Smartt, S. J. 2016, ApJ, 831, 79
Inserra, C., Nicholl, M., Chen, T.-W., et al. 2017, MNRAS, 468, 4642
Inserra, C., Prajs, S., Gutierrez, C. P., et al. 2018a, ApJ, 854, 175
Inserra, C., Smartt, S. J., Gall, E. E. E., et al. 2018b, MNRAS, 475, 1046
Ioka, K., Hotokezaka, K., & Piran, T. 2016, ApJ, 833, 110
Izzo, L., Thöne, C. C., García-Benito, R., et al. 2018, A&A, 610, A11
Izzo, L., de Ugarte Postigo, A., Maeda, K., et al. 2019, Nature, 565, 324
Janiuk, A., Charzyński, S., & Bejger, M. 2013a, A&A, 560, A25
Janiuk, A., Charzyński, S., & Mioduszewski, P. 2013b, Mem. Soc. Astron. It., 84, 727
Jerkstrand, A., Smartt, S. J., Inserra, C., et al. 2017, ApJ, 835, 13
Kangas, T., Blagorodnova, N., Mattila, S., et al. 2017, MNRAS, 469, 1246
Kann, D. A., Klose, S., & Zeh, A. 2006, ApJ, 641, 993
Kann, D. A., Masetti, N., & Klose, S. 2007, AJ, 133, 1187
Kann, D. A., Klose, S., Zhang, B., et al. 2010, ApJ, 720, 1513
Kann, D. A., Klose, S., Zhang, B., et al. 2011, ApJ, 734, 96
Kann, D. A., de Ugarte Postigo, A., Izzo, L., & Thoene, C. C. 2017, GRBCoordinates Network, Circular Service, 21345, 21345
Kann, D. A., Schady, P., Olivares, E. F., et al. 2018, A&A, 617, A122
Kasen, D., Metzger, B. D., & Bildsten, L. 2016, ApJ, 821, 36
Kashiyama, K., Nakauchi, D., Suwa, Y., Yajima, H., & Nakamura, T. 2013, ApJ, 770, 8
Klose, S., Schmidl, S., Kann, D. A., et al. 2019, A&A, 622, A138
Kostrzewa-Rutkowska, Z., Kozłowski, S., Wyrzykowski, Ł., et al. 2013, ApJ, 778, 168
Kouveliotou, C., Meegan, C. A., Fishman, G. J., et al. 1993, ApJ, 413, L101
Kozyreva, A., Hirschi, R., Blinnikov, S., & den Hartogh, J. 2016, MNRAS, 459, L21
Krühler, T., Malesani, D., Fynbo, J. P. U., et al. 2015, A&A, 581, A125
Krühler, T., Kuncarayakti, H., Schady, P., et al. 2017, A&A, 602, A85
Krühler, T., Fraser, M., Leloudas, G., et al. 2018, A&A, 610, A14
Kuncarayakti, H., Maeda, K., Ashall, C. J., et al. 2018, ApJ, 854, L14
Leloudas, G., Chatzopoulos, E., Dilday, B., et al. 2012, A&A, 541, A129
Leloudas, G., Schulze, S., Krühler, T., et al. 2015a, MNRAS, 449, 917
Leloudas, G., Patat, F., Maund, J. R., et al. 2015b, ApJ, 815, L10
Leloudas, G., Fraser, M., Stone, N. C., et al. 2016, Nat. Astron., 1, 0002
Leloudas, G., Maund, J. R., Gal-Yam, A., et al. 2017, ApJ, 837, L14
Levan, A. J. 2015, J. High Energy Astrophys., 7, 44
Levan, A. J., Tanvir, N. R., Cenko, S. B., et al. 2011, Science, 333, 199
Levan, A. J., Read, A. M., Metzger, B. D., Wheatley, P. J., & Tanvir, N. R. 2013, ApJ, 771, 136

Levan, A. J., Tanvir, N. R., Starling, R. L. C., et al. 2014, ApJ, 781, 13
Liu, L.-D., Wang, S.-Q., Wang, L.-J., et al. 2017a, ApJ, 842, 26
Liu, Y.-Q., Modjaz, M., & Bianco, F. B. 2017b, ApJ, 845, 85
Liu, L.-D., Wang, L.-J., Wang, S.-Q., & Dai, Z.-G. 2018a, ApJ, 856, 59
Liu, T., Song, C.-Y., Zhang, B., Gu, W.-M., & Heger, A. 2018b, ApJ, 852, 20
Lü, H.-J., & Zhang, B. 2014, ApJ, 785, 74
Lunnan, R., Chornock, R., Berger, E., et al. 2013, ApJ, 771, 97
Lunnan, R., Chornock, R., Berger, E., et al. 2014, ApJ, 787, 138
Lunnan, R., Chornock, R., Berger, E., et al. 2016, ApJ, 831, 144
Lunnan, R., Chornock, R., Berger, E., et al. 2018a, ApJ, 852, 81
Lunnan, R., Fransson, C., Vreeswijk, P. M., et al. 2018b, Nat. Astron., 2, 887
Lyman, J. D., Bersier, D., James, P. A., et al. 2016, MNRAS, 457, 328
Maeda, K., Mazzali, P. A., Deng, J., et al. 2003, ApJ, 593, 931
Malesani, D., Fynbo, J. P. U., Hjorth, J., et al. 2009, ApJ, 692, L84
Margalit, B., Metzger, B. D., Berger, E., et al. 2018a, MNRAS, 481, 2407
Margalit, B., Metzger, B. D., Thompson, T. A., Nicholl, M., & Sukhbold, T. 2018b, MNRAS, 475, 2659
Margutti, R., Milisavljevic, D., Soderberg, A. M., et al. 2014, ApJ, 797, 107
Margutti, R., Guidorzi, C., Lazzati, D., et al. 2015, ApJ, 805, 159
Margutti, R., Metzger, B. D., Chornock, R., et al. 2017, ApJ, 836, 25
Margutti, R., Chornock, R., Metzger, B. D., et al. 2018, ApJ, 864, 45
Masetti, N., Palazzi, E., Pian, E., et al. 2003, A&A, 404, 465
Mauerhan, J. C., Filippenko, A. V., Zheng, W., et al. 2018, MNRAS, 478, 5050
Maund, J. R., Steele, I., Jermak, H., Wheeler, J. C., & Wiersema, K. 2019, MNRAS, 482, 4057
Mazets, E. P., Golenetskii, S. V., Ilinskii, V. N., et al. 1981, Ap&SS, 80, 3
Mazzali, P. A., Deng, J., Nomoto, K., et al. 2006, Nature, 442, 1018
Mazzali, P. A., Valenti, S., Della Valle, M., et al. 2008, Science, 321, 1185
Mazzali, P. A., Sullivan, M., Pian, E., Greiner, J., & Kann, D. A. 2016, MNRAS, 458, 3455
McCrum, M., Smartt, S. J., Kotak, R., et al. 2014, MNRAS, 437, 656
McCrum, M., Smartt, S. J., Rest, A., et al. 2015, MNRAS, 448, 1206
McKenzie, E. H., & Schaefer, B. E. 1999, PASP, 111, 964
Melandri, A., Pian, E., D'Elia, V., et al. 2014, A&A, 567, A29
Metzger, B. D., Giannios, D., Thompson, T. A., Bucciantini, N., & Quataert, E. 2011, MNRAS, 413, 2031
Metzger, B. D., Margalit, B., Kasen, D., & Quataert, E. 2015, MNRAS, 454, 3311
Metzger, B. D., Beniamini, P., & Giannios, D. 2018, ApJ, 857, 95
Milisavljevic, D., Soderberg, A. M., Margutti, R., et al. 2013, ApJ, 770, L38
Milisavljevic, D., Margutti, R., Parrent, J. T., et al. 2015a, ApJ, 799, 51
Milisavljevic, D., Margutti, R., Kamble, A., et al. 2015b, ApJ, 815, 120
Moriya, T., Tominaga, N., Tanaka, M., Maeda, K., & Nomoto, K. 2010, ApJ, 717, L83
Moriya, T. J., Metzger, B. D., & Blinnikov, S. I. 2016, ApJ, 833, 64
Moriya, T. J., Sorokina, E. I., & Chevalier, R. A. 2018, Space Sci. Rev., 214, 59
Moriya, T. J., Tanaka, M., Yasuda, N., et al. 2019, ApJS, 241, 16
Mould, J. R., Huchra, J. P., Freedman, W. L., et al. 2000, ApJ, 529, 786
Nakauchi, D., Kashiyama, K., Suwa, Y., & Nakamura, T. 2013, ApJ, 778, 67
Nathanail, A., & Contopoulos, I. 2015, MNRAS, 453, L1
Nicholl, M., Smartt, S. J., Jerkstrand, A., et al. 2013, Nature, 502, 346
Nicholl, M., Smartt, S. J., Jerkstrand, A., et al. 2014, MNRAS, 444, 2096
Nicholl, M., Smartt, S. J., Jerkstrand, A., et al. 2015a, ApJ, 807, L18
Nicholl, M., Smartt, S. J., Jerkstrand, A., et al. 2015b, MNRAS, 452, 3869
Nicholl, M., Berger, E., Margutti, R., et al. 2016a, ApJ, 828, L18
Nicholl, M., Berger, E., Smartt, S. J., et al. 2016b, ApJ, 826, 39
Nicholl, M., Guillochon, J., & Berger, E. 2017a, ApJ, 850, 55
Nicholl, M., Berger, E., Margutti, R., et al. 2017b, ApJ, 835, L8
Nicholl, M., Berger, E., Margutti, R., et al. 2017c, ApJ, 845, L8
Olivares, E. F., Greiner, J., Schady, P., et al. 2012, A&A, 539, A76
Olivares, E. F., Greiner, J., Schady, P., et al. 2015, A&A, 577, A44
Papadopoulos, A., D'Andrea, C. B., Sullivan, M., et al. 2015, MNRAS, 449, 1215
Pastorello, A., Smartt, S. J., Botticella, M. T., et al. 2010, ApJ, 724, L16
Perets, H. B., Li, Z., Lombardi, Jr., J. C., & Milcarek, Jr., S. R. 2016, ApJ, 823, 113
Perley, D. A., Cenko, S. B., Corsi, A., et al. 2014, ApJ, 781, 37
Perley, D. A., Quimby, R. M., Yan, L., et al. 2016, ApJ, 830, 13
Perna, R., Lazzati, D., & Cantiello, M. 2018, ApJ, 859, 48
Petropoulou, M., Barniol Duran, R., & Giannios, D. 2017, MNRAS, 472, 2722
Pian, E., Mazzali, P. A., Masetti, N., et al. 2006, Nature, 442, 1011
Pignata, G., Stritzinger, M., Soderberg, A., et al. 2011, ApJ, 728, 14
Piran, T., Nakar, E., Mazzali, P., & Pian, E. 2019, ApJ, 871, L25
Prentice, S. J., Mazzali, P. A., Pian, E., et al. 2016, MNRAS, 458, 2973
Prentice, S. J., & Mazzali, P. A. 2017, MNRAS, 469, 2672
Prentice, S. J., Ashall, C., James, P. A., et al. 2018, MNRAS, 484, 2692
Price, P. A., Kulkarni, S. R., Berger, E., et al. 2003, ApJ, 589, 838
Quataert, E., & Kasen, D. 2012, MNRAS, 419, L1
Quimby, R. M., Kulkarni, S. R., Kasliwal, M. M., et al. 2011, Nature, 474, 487
Quimby, R. M., Yuan, F., Akerlof, C., & Wheeler, J. C. 2013, MNRAS, 431, 912
Quimby, R. M., De Cia, A., Gal-Yam, A., et al. 2018, ApJ, 855, 2
Racusin, J. L., Karpov, S. V., Sokolowski, M., et al. 2008, Nature, 455, 183
Renault-Tinacci, N., Kotera, K., Neronov, A., & Ando, S. 2018, A&A, 611, A45
Rest, A., Foley, R. J., Gezari, S., et al. 2011, ApJ, 729, 88
Richardson, D., Jenkins, III., R. L., Wright, J., & Maddox, L. 2014, AJ, 147, 118
Roy, R., Sollerman, J., Silverman, J. M., et al. 2016, A&A, 596, A67
Sana, H., de Mink, S. E., de Koter, A., et al. 2012, Science, 337, 444
Sanders, N. E., Soderberg, A. M., Valenti, S., et al. 2012, ApJ, 756, 184
Schlafly, E. F., & Finkbeiner, D. P. 2011, ApJ, 737, 103
Schulze, S., Malesani, D., Cucchiara, A., et al. 2014, A&A, 566, A102
Schulze, S., Krühler, T., Leloudas, G., et al. 2018, MNRAS, 473, 1258
Siegel, M. H., Evans, P. A., Oates, S. R. N., Burrows, S. D., & Gehrels, N. 2013, GCN Report, 410
Smartt, S. J. 2009, ARA&A, 47, 63
Smith, M., Sullivan, M., D'Andrea, C. B., et al. 2016, ApJ, 818, L8
Smith, R. M., Dekany, R. G., Bebek, C., et al. 2014, SPIE Conf. Ser., 9147, 79
Sobacchi, E., Granot, J., & Bromberg, O. 2017a, ArXiv e-prints [arXiv:1705.00792]
Sobacchi, E., Granot, J., Bromberg, O., & Sormani, M. C. 2017b, MNRAS, 472, 616
Soderberg, A. M., Berger, E., Page, K. L., et al. 2008, Nature, 453, 469
Soderberg, A. M., Chakraborti, S., Pignata, G., et al. 2010, Nature, 463, 513
Soker, N., & Gilkis, A. 2017, ApJ, 851, 95
Sollerman, J., Fynbo, J. P. U., Gorosabel, J., et al. 2007, A&A, 466, 839
Sonbas, E., MacLachlan, G. A., Dhuga, K. S., et al. 2015, ApJ, 805, 86
Song, C.-Y., & Liu, T. 2019, ApJ, 871, 117
Spergel, D. N., Verde, L., Peiris, H. V., et al. 2003, ApJS, 148, 175
Stanek, K. Z., Matheson, T., Garnavich, P. M., et al. 2003, ApJ, 591, L17
Stanek, K. Z., Garnavich, P. M., Nutzman, P. A., et al. 2005, ApJ, 626, L5
Stratta, G., Gendre, B., Atteia, J. L., et al. 2013, ApJ, 779, 66
Stritzinger, M. D., Anderson, J. P., Contreras, C., et al. 2018a, A&A, 609, A134
Stritzinger, M. D., Taddia, F., Burns, C. R., et al. 2018b, A&A, 609, A135
Suntzeff, N. B., & Bouchet, P. 1990, AJ, 99, 650
Suwa, Y., & Tominaga, N. 2015, MNRAS, 451, 282
Suzuki, A., & Maeda, K. 2017, MNRAS, 466, 2633
Taddia, F., Stritzinger, M. D., Bersten, M., et al. 2018, A&A, 609, A136
Taddia, F., Sollerman, J., Fremling, C., et al. 2019a, A&A, 621, A71
Taddia, F., Sollerman, J., Fremling, C., et al. 2019b, A&A, 621, A64
Thöne, C. C., de Ugarte Postigo, A., Fryer, C. L., et al. 2011, Nature, 480, 72
Thöne, C. C., de Ugarte Postigo, A., García-Benito, R., et al. 2015, MNRAS, 451, L65
Tolstov, A., Zhiglo, A., Nomoto, K., et al. 2017, ApJ, 845, L2
Tominaga, N., Deng, J., Mazzali, P. A., et al. 2004, ApJ, 612, L105
Toy, V. L., Cenko, S. B., Silverman, J. M., et al. 2016, ApJ, 818, 79
Troja, E., Cusumano, G., O'Brien, P. T., et al. 2007, ApJ, 665, 599
Tyson, J. A. 2002, in Survey and Other Telescope Technologies and Discoveries, eds. J. A. Tyson, & S. Wolff, SPIE Conf. Ser., 4836, 10
Vallely, P. J., Prieto, J. L., Stanek, K. Z., et al. 2018, MNRAS, 475, 2344
Vergani, S. D., Flores, H., Covino, S., et al. 2011, A&A, 535, A127
Vreeswijk, P. M., Savaglio, S., Gal-Yam, A., et al. 2014, ApJ, 797, 24
Vreeswijk, P. M., Leloudas, G., Gal-Yam, A., et al. 2017, ApJ, 835, 58
Walker, E. S., Mazzali, P. A., Pian, E., et al. 2014, MNRAS, 442, 2768
Wang, S.-Q., Liu, L.-D., Dai, Z.-G., Wang, L.-J., & Wu, X.-F. 2016a, ApJ, 828, 87
Wang, L.-J., Han, Y.-H., Xu, D., et al. 2016b, ApJ, 831, 41
Wang, S.-Q., Cano, Z., Wang, L.-J., et al. 2017a, ApJ, 850, 148
Wang, L.-J., Yu, H., Liu, L.-D., et al. 2017b, ApJ, 837, 128
Wang, L.-J., Cano, Z., Wang, S.-Q., et al. 2017c, ApJ, 851, 54
Whitesides, L., Lunnan, R., Kasliwal, M. M., et al. 2017, ApJ, 851, 107
Woosley, S. E., & Heger, A. 2012, ApJ, 752, 32
Woosley, S. E., Eastman, R. G., & Schmidt, B. P. 1999, ApJ, 516, 788
Wright, E. L. 2006, PASP, 118, 1711
Yan, L., Quimby, R., Ofek, E., et al. 2015, ApJ, 814, 108
Yan, L., Lunnan, R., Perley, D. A., et al. 2017, ApJ, 848, 6
Yan, L., Perley, D. A., De Cia, A., et al. 2018, ApJ, 858, 91
Yoon, S.-C., & Langer, N. 2005, A&A, 443, 643
Yu, Y.-W., Zhu, J.-P., Li, S.-Z., Lü, H.-J., & Zou, Y.-C. 2017, ApJ, 840, 12
Zeh, A., Klose, S., & Hartmann, D. H. 2004, ApJ, 609, 952
Zhang, B., & Mészáros, P. 2001, ApJ, 552, L35
Zhang, B., Zhang, B.-B., Liang, E.-W., et al. 2007, ApJ, 655, L25
Zhang, B., Zhang, B.-B., Virgili, F. J., et al. 2009, ApJ, 703, 1696
Zhang, B.-B., Burrows, D. N., Zhang, B., et al. 2012, ApJ, 748, 132

[1] Thüringer Landessternwarte Tautenburg, Sternwarte 5, 07778 Tautenburg, Germany
e-mail: kann@iaa.es
[2] Max-Planck-Institut für extraterrestrische Physik, Giessenbachstraße 1, 85748 Garching, Germany
[3] Universe Cluster, Technische Universität München, Boltzmannstraße 2, 85748 Garching, Germany
[4] Instituto de Astrofísica de Andalucía (IAA-CSIC), Glorieta de la Astronomía s/n, 18008 Granada, Spain
[5] Departamento de Ciencias Fisicas, Universidad Andres Bello, Avda. Republica 252, Santiago, Chile
[6] INAF-IASF Bologna, Area della Ricerca CNR, Via Gobetti 101, 40129 Bologna, Italy
[7] Cahill Center for Astrophysics, California Institute of Technology, Pasadena, CA 91125, USA
[8] Dark Cosmology Centre, Niels Bohr Institute, University of Copenhagen, Juliane Maries Vej 30, 2100 Copenhagen, Denmark
[9] Astrophysics Research Institute, Liverpool John Moores University, IC2, Liverpool Science Park, 146 Brownlow Hill, Liverpool L3 5RF, UK
[10] ESO, Alonso de Cordova 3107, Vitacura, Santiago de Chile, Chile
[11] Harvard-Smithsonian Center for Astrophysics, 60 Garden St., Cambridge, MA 02138, USA
[12] Institute of Experimental and Applied Physics, Czech Technical University in Prague, Horská 3a/22, 12800 Prague, Czech Republic
[13] Scuola Normale Superiore, Piazza dei Cavalieri 7, 56126 Pisa, Italy
[14] Astrophysics Research Institute, Liverpool John Moores University, 146 Brownlow Hill, Liverpool L3 5RF, UK
[15] Max-Planck Institut für Astrophysik, Karl-Schwarzschild-Str. 1, 85748 Garching, Germany
[16] Department of Particle Physics & Astrophysics, Weizmann Institute of Science, Rehovot 76100, Israel
[17] American River College, Physics and Astronomy Dpt., 4700 College Oak Drive, Sacramento, CA 95841, USA
[18] Instituto de Astrofísica, Facultad de Física, Pontificia Universidad Católica de Chile, Av. Vicuña Mackenna 4860, 306, Santiago 22, Chile
[19] Millennium Institute of Astrophysics, Av. Vicuña Mackenna 4860, 7820436 Macul, Santiago, Chile
[20] Department of Particle Physics and Astrophysics, Faculty of Physics, Weizmann Institute of Science, Rehovot 76100, Israel
[21] Department of Chemistry and Physics, Roger Williams University, One Old Ferry Road, Bristol, RI 02809, USA

Appendix A: Data sources for Fig. 4

GRB-SNe: Olivares et al. (2012, 2015), Schulze et al. (2014), Toy et al. (2016), Ashall et al. (2017), Cano et al. (2017b), Corsi et al. (2017), de Ugarte Postigo et al. (2017), Izzo et al. (2019).

Gap transients and others: Arcavi et al. (2016), Roy et al. (2016), Vallely et al. (2018), Whitesides et al. (2017), Benetti et al. (2018), Chen et al. (2018), Kann et al. (in prep).

SLSNe: Quimby et al. (2011), Chomiuk et al. (2011), Rest et al. (2011), Leloudas et al. (2012), Cooke et al. (2012), Chatzopoulos et al. (2013), Kostrzewa-Rutkowska et al. (2013), Howell et al. (2013), Nicholl et al. (2013, 2014, 2015a, 2016b, 2017b), Lunnan et al. (2013, 2016, 2018a,b), Inserra et al. (2013, 2018b, 2017), Benetti et al. (2014), Vreeswijk et al. (2014, 2017), McCrum et al. (2014, 2015), Papadopoulos et al. (2015), Yan et al. (2015, 2017), Smith et al. (2016), Chen et al. (2017b), De Cia et al. (2018), Blanchard et al. (2018, 2019), Anderson et al. (2018), Taddia et al. (2019a), Angus et al. (2018).

ASASSN-15lh: Dong et al. (2016).

Appendix B: Erratum to K18B

In K18B, we measured the offset between GRB 111209A/SN 2011kl and the centre of its host galaxy. Hereby, the correction for the cosine of the rectascension was not implemented. With this additional term, we find an offset in RA of 0.″271, and therefore a total offset of 0.″33 ± 0.″18, which translates to a projected offset of 2.26 ± 1.25 kpc. This is in better agreement with the result of L14, and otherwise does not change our conclusions.